METEOROLOGISKA INSTITUTET
FINNISH METEOROLOGICAL INSTITUTE

FINNISH METEOROLOGICAL INSTITUTE

85

CONTRIBUTIONS

EVALUATION AND APPLICATION OF PASSIVE AND ACTIVE OPTICAL REMOTE SENSING METHODS FOR THE MEASUREMENT OF ATMOSPHERIC AEROSOL PROPERTIES

TERO MIELONEN

EVALUATION AND APPLICATION OF PASSIVE AND ACTIVE OPTICAL REMOTE SENSING METHODS FOR THE MEASUREMENT OF ATMOSPHERIC AEROSOL PROPERTIES

Tero Mielonen

Department of Physics and Mathematics
University of Eastern Finland
Kuopio, Finland

Doctoral dissertation

To be presented, with the permission of the Faculty of Science and Forestry of the University of Eastern Finland for public examination in Auditorium L1, Canthia building, University of Eastern Finland, on November 19th, 2010, at 12 noon.

FINNISH METEOROLOGICAL INSTITUTE

Author
Tero Mielonen

Name of project

Commissioned by

Title
EVALUATION AND APPLICATION OF PASSIVE AND ACTIVE OPTICAL REMOTE SENSING METHODS FOR THE MEASUREMENT OF ATMOSPHERIC AEROSOL PROPERTIES

Abstract

Atmospheric aerosol particles affect the atmosphere's radiation balance by scattering and absorbing sunlight. Moreover, the particles act as condensation nuclei for clouds and affect their reflectivity. In addition, aerosols have negative health effects and they reduce visibility. Aerosols are emitted into the atmosphere from both natural and anthropogenic sources. Different types of aerosols have different effects on the radiation balance, thus global monitoring and typing of aerosols is of vital importance.

In this thesis, several remote sensing methods used in the measurement of atmospheric aerosols are evaluated. Remote sensing of aerosols can be done with active and passive instruments. Passive instruments measure radiation emitted by the sun and the Earth while active instruments have their own radiation source, for example a black body radiator or a laser. The instruments utilized in these studies were sun photometers (PFR, Cimel), lidars (Polly^{XT}, CALIOP), transmissometer (OLAF) and a spectroradiometer (MODIS). Retrieval results from spaceborne instruments (MODIS, CALIOP) were evaluated with ground based measurements (PFR, Cimel). In addition, effects of indicative aerosol model assumptions on the calculated radiative transfer were studied. Finally, aerosol particle mass at the ground level was approximated from satellite measurements and vertical profiles of aerosols measured with a lidar were analyzed.

For the evaluation part, these studies show that the calculation of aerosol induced attenuation of radiation based on aerosol size distribution measurements is not a trivial task. In addition to dry aerosol size distribution, the effect of ambient relative humidity on the size distribution and the optical properties of the aerosols need to be known in order to achieve correct results form the calculations. Furthermore, the results suggest that aerosol size parameters retrieved from passive spaceborne measurements depend heavily on surface reflectance assumptions and more realistic assumptions improve the retrieved parameters. However, other derived parameters, i.e. aerosol optical depth may deteriorate. In addition, the possibility to improve aerosol typing based on active spaceborne measurements by adding an additional parameter into the retrieval was studied. Unfortunately, the available parameter (color ratio) did not bring additional information into the retrieval. For the application part, remote sensed data was used in the estimation of particulate matter at the surface and in the analysis of seasonal profiles of vertical properties.

The studies in this thesis show that optical remote sensing can give invaluable information on the properties of atmospheric aerosols. However, the retrieval of aerosol properties with underdetermined information content is an extremely difficult task. Thus, the user should be aware of the uncertainties and the error sources in the retrieved parameters.

ILMATIETEEN LAITOS

Tekijä(t)
Tero Mielonen

Projektin nimi

Toimeksiantaja

Nimeke
PASSIIVISTEN JA AKTIIVISTEN KAUKOKARTOITUSMENETELMIEN KÄYTETTÄVYYS ILMAKEHÄN AEROSOLIEN OMINAISUUKSIEN MITTAUKSESSA

Tiivistelmä

Ilmakehässä olevat pienhiukkaset vaikuttavat ilmakehän säteilytasapainoon sirottamalla ja absorboimalla auringon valoa. Lisäksi ne toimivat pilvien tiivistymisytiminä vaikuttaen pilvien kykyyn heijastaa säteilyä. Pienhiukkasilla on myös haitallisia terveysvaikutuksia ja ne heikentävät näkyvyyttä. Pienhiukkasia pääsee ilmakehään sekä luonnollisista lähteistä, kuten tulivuoren purkauksista, että ihmistoiminnan seurauksena, kuten liikenteestä ja teollisuudesta. Eri lähteistä syntyneillä hiukkasilla on erilaiset ominaisuudet ja ne vaikuttavat eri tavalla ilmakehän säteilytasapainoon, minkä vuoksi hiukkasten maailmanlaajuinen seuranta on tärkeää.

Tässä väitöskirjassa arvioitiin aktiivisten ja passiivisten kaukokartoitusmenetelmien käytettävyyttä ilmakehän pienhiukkasten seurannassa. Passiiviset instrumentit mittaavat auringon ja maan lähettämää säteilyä, kun taas aktiiviset laitteet tuottavat mittaussignaalin itse esimerkiksi mustankappaleen säteilyllä tai laserilla. Tutkimuksessa hyödynnettiin fotometreillä (PFR, Cimel), lidareilla (Polly^{XT}, CALIOP), transmissometrillä (OLAF) ja spektraalisella säteilymittarilla (MODIS) tehtyjä optisia mittauksia. Satelliiteista tehtyjen havaintojen (MODIS, CALIOP) laatua arvioitiin maanpinnalta tehtyjen mittausten avulla (PFR, Cimel). Lisäksi tutkittiin satelliittialgoritmeissa käytettyjen oletusten vaikutusta säteilynkulun mallintamiseen. Lopuksi arvioitiin pienhiukkasten massapitoisuutta maanpinnalla satelliittimittauksista ja analysoitiin lidar-mittauksista saatuja pienhiukkasten pystyprofiileja.

Tutkimus osoitti, että mitattujen hiukkaskokojakaumien pohjalta on haastavaa laskea pienhiukkasten aiheuttaman säteilyn vaimeneminen. Luotettavan tuloksen saamiseksi on tunnettava paitsi hiukkasten kuiva kokojakauma myös ilman suhteellisen kosteuden vaikutus kokojakaumaan sekä hiukkasten optiset ominaisuudet. Lisäksi tulokset osoittivat, että satelliittialgoritmeissa tehdyt oletukset maanpinnan heijastuvuudesta vaikuttavat merkittävästi passiivisista satelliittimittauksista saatuihin aerosolien kokoparametreihin. Realistisemmat oletukset parantavat kokoparametria, mutta muiden parametrien, kuten aerosolien optisen paksuuden, tarkkuus voi jopa heiketä. Tutkimuksessa kehitettiin myös menetelmä, jolla voidaan arvioida aktiivisesta satelliittimittauksesta saatavan pienhiukkasten tyyppiluokittelun luotettavuutta. Tyyppiluokittelussa havaittiin puutteita, joten sen parantamista tutkittiin lisäämällä algoritmiin ylimääräinen parametri. Tämä (color ratio) ei kuitenkaan tuonut algoritmiin olennaista lisätietoa pienhiukkasten tyypeistä. Kaukokartoitusmittauksia hyödynnettiin maanpinnalla olevien pienhiukkaspitoisuuksien arvioinnissa ja niiden ominaisuuksien pystyprofiilin määrittämisessä. Tulokset osoittivat, että Suomen olosuhteissa maanpinnalla olevia pienhiukkaspitoisuuksia voidaan arvioida satelliittimittauksista. Pienhiukkasten pystyprofiilien vuodenaikaiskeskiarvot Gual Paharista, Intiasta paljastivat selkeitä eroja eri vuodenaikojen välillä.

Optinen kaukokartoitus tuottaa tärkeää tietoa ilmakehän pienhiukkasista. Mittaukset ovat kuitenkin vaativia ja tulokset ovat herkkiä virhetulkinnoille, minkä vuoksi mittaustiedon käyttäjän on tunnettava mittauksiin liittyvät rajoitukset ja epävarmuudet.

Acknowledgments

CONTENTS

LIST OF ORIGINAL PUBLICATIONS

This thesis consists of an Introduction and five original papers:

Paper I: Mielonen, T., T. Kaurila, A. Arola, H. Lihavainen, and K. E. J. Lehtinen, Effect of Aerosols on the Infrared transmission in Lakiala, Finland, *Atmos. Environ.*, **42**, 2603–2610, doi:10.1016/j.atmosenv.2007.09.038, 2008.

Paper II: Mielonen, T., R. C. Levy, V. Aaltonen, M. Komppula, G. de Leeuw, J. Huttunen, H. Lihavainen, P. Kolmonen, K. E. J. Lehtinen, and A. Arola, Evaluating the assumptions of surface reflectance and aerosol type selection within the MODIS aerosol retrieval over land: the problem of dust type selection, *Atmos. Meas. Tech. Disc.*, **3**, 3425–3453, doi:10.5194/amtd-3-3425-2010, **Submitted**, 2010 (version corrected according to referee comments).

Paper III: Mielonen, T., A. Arola, M. Komppula, J. Kukkonen, J. Koskinen, G. de Leeuw, and K. E. J. Lehtinen, Comparison of CALIOP level 2 aerosol subtypes to aerosol types derived from AERONET inversion data, *Geophys. Res. Lett.*, **36**, L18804, doi:10.1029/2009GL039609, 2009.

Paper IV: Natunen, A., A. Arola, T. Mielonen, J. Huttunen, M. Komppula, and K. E. J. Lehtinen, A multi-year comparison of $PM_{2.5}$ and AOD for the Helsinki region, *Boreal. Env. Res.*, **15**, 544–552, 2010.

Paper V: Komppula M., T. Mielonen, A. Arola, K. Korhonen, H. Lihavainen, A.-P. Hyvärinen, H. Baars, R. Engelmann, D. Althausen, A. Ansmann, D. Müller, T. S. Panwar, R. K. Hooda, V. P. Sharma, V.-M. Kerminen, K. E. J. Lehtinen, and Y. Viisanen, One year of raman-lidar measurements in Gual Pahari close to New Delhi India: Seasonal characteristics of the aerosol vertical structure, *Atmos. Chem. Phys. Disc.*, **Submitted**, 2010.

T. Mielonen is responsible for the major work, as well as for the manuscript writing in Papers I, II and III. In Paper IV T. Mielonen is responsible for the data analysis together with A. Natunen and writing of the manuscript in the revision stage. In Paper V T. Mielonen is responsible for the calculation of the lidar profiles, and for related writing of the manuscript.

1 INTRODUCTION

Aerosols play an important role in the Earth's atmosphere. They affect, for example, radiation budget, cloud processes and air quality. The direct effect of aerosols on climate involves both scattering and absorption of radiation, while the indirect effect of aerosols is related to their ability to modify the optical properties and lifetimes of clouds. Immense amounts of work has been done to study aerosol's climate effects (e.g. Charlson et al. (1992); Penner (1992); Dickerson et al. (1997); Bréon et al. (2002); Chung et al. (2010); Chen W.-T. et al. (2010); Quaas et al. (2010); Lubin and Vogelmann (2010)). However, aerosols still have the largest uncertainty in the climate change modeling (IPCC (2007); Schwartz et al. (2010)). In addition to the radiative effects, aerosols influence air quality and visibility which also have significant effects on people's daily life. Several studies have shown that exposure to high concentrations of particulate matter contributes to public morbidity, mortality of respiratory and cardiovascular diseases (e.g., Pope (2000); Wallace (2000); Kan and Chen (2002); Li et al. (2006)).

Due to these effects it is important to monitor, model and forecast aerosol amounts and properties. In-situ measurements from all atmospheric aerosol layers are difficult to make because the layers are typically lofted and there can be multiple layers with different properties. Only instruments situated in towers and airplanes can measure off the ground aerosol layers. However, these kind of measurements are available only from specific sites and times. With remote sensing instruments aerosol properties can be derived for troposphere and stratosphere. Moreover, instruments aboard satellites provide data from all over the globe.

Remote sensing methods have a huge potential in aerosol science. In addition to climate studies, they can be used in air quality monitoring and plume tracking. For example, satellite and lidar measurements provided valuable data on the ash plume from the Eyjafjällajökull volcano eruption (e.g. de Leeuw et al. (2010); Ansmann et al. (2010)). In climate change research, remote sensing data is ideal for model validation and assimilation (e.g. Quaas et al. (2009)).

The aim of this research was to evaluate and apply various optical remote sensing methods for the measurement of atmospheric aerosols over land. The main objectives of this thesis were to

1. evaluate the aerosol properties (e.g. amount of aerosols and their size) derived from the studied remote sensing instruments and study the restrictions of these measurements, especially over land

2. find ways to improve the aerosol retrievals done with the remote sensing instruments under study

3. use satellite and lidar measurements to study regional aerosol properties (e.g. amount of aerosols and their vertical profiles)

The thesis consists of 5 original papers, which will be referred by roman numerals (I-V). The major contributions of the papers are as follows.

In Paper I aerosol extinction coefficients measured with a transmissometer and modeled with a radiative transfer code (MODTRAN4) are studied as a function of weather parameters (visibility, relative humidity and temperature). In addition, measured size distributions are investigated and they are compared with the size distribution assumed in the radiative transfer code. The effect of aerosols on radiative transfer depends on their size distribution and optical properties. Typically, the algorithms used in remote sensing retrievals have to assume these properties and the errors in the assumptions affect the quality of the retrieved products.

In Paper II Aerosol Optical Depth (AOD) and Ångström exponent (AE) values derived with the Moderate Resolution Imaging Spectroradiometer (MODIS) retrieval algorithm over land are compared with ground based sun photometer measurements in Europe, Asia, Africa North America and South America. Furthermore, the possible reasons (assumptions in the retrieval algorithm) for the discrepancies between the satellite and ground based measurements are analyzed and a method to improve MODIS AE retrieval is presented.

In Paper III the aerosol subtypes of space borne lidar (CALIOP) measurements are compared with daily aerosol types derived from sun photometer inversion data. A method to evaluate the quality of the CALIOP aerosol type classification is presented. The simplified aerosol typing with the sun photometer data is based on AE and Single Scattering Albedo (SSA) values. Identification of aerosol types (in terms of their source origin and main composition) is important because of the effects that different aerosols have on health, visibility and Earth's climate.

In Paper IV MODIS AOD measurements are compared with ground based particle mass ($PM_{2.5}$) measurements done at four sites near each other in Helsinki, Finland. Three of the sites represent urban environment while one is from a rural area. The effect of temporal $PM_{2.5}$ averaging on the correlation between AOD and $PM_{2.5}$ is investigated. In addition, the seasonality of the correlation is studied. Moreover, conversion factors which could be used to estimate $PM_{2.5}$ from AOD in this region are presented.

In Paper V one year (March 2008 to March 2009) of ground-based Raman lidar measurements done in Gual Pahari, India are analyzed. This is the longest lidar data set available from New Delhi. Close to 500 one-hour profiles are averaged from 183 measurement days. From them, seasonal profiles of aerosol backscattering, extinction, lidar ratios and AE are calculated and compared with results from other studies.

2 THEORETICAL CONCEPTS

Electromagnetic radiation is the most important process responsible for energy transfer in the atmosphere. This radiation travels in wave form, and all electromagnetic waves travel at the speed of light (2.99793×10^8 m/s) in a vacuum. In the air, the speed is nearly the same. Visible light, gamma rays, x-rays, ultraviolet radiation, infrared radiation, microwaves, and radio waves constitute the electromagnetic spectrum. These types can be separated based on their *wavelength*, which is the distance over which the wave's shape repeats. The human eye is sensitive to electromagnetic radiation whose wavelength is between 390 nm and 750 nm. Electromagnetic radiation with shorter wavelengths (10 nm – 400 nm) is called ultraviolet radiation, while radiation with longer wavelengths (0.7 μm – 10 μm) is called infrared radiation (Liou, 2002). We can feel infrared radiation as heat but ultraviolet radiation is beyond our senses.

In remote sensing, information (spectral, spatial, temporal) about objects is acquired without coming into physical contact with the objects under investigation. In-
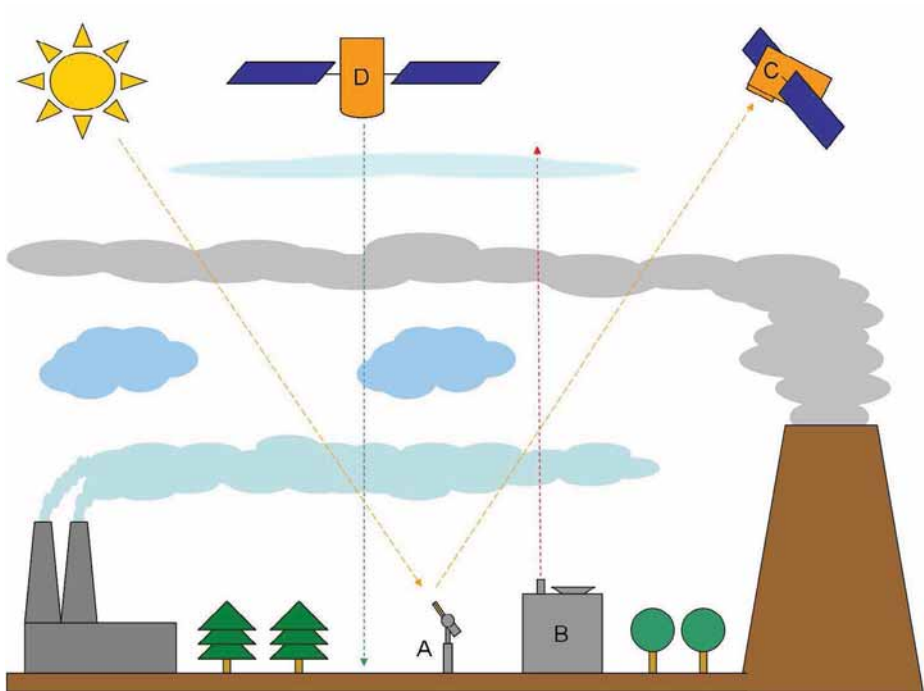

Figure 2.1. Measurement principles for ground-based (A and B) and spaceborne remote sensing (C and D) instruments. A and C are passive instruments which measure radiation coming from the sun, while B and D are active instruments which have their own signal source, e.g. laser.

formation transfer is accomplished by the use of electromagnetic radiation. The interpretation and inversion of the measurements require the use of fundamental light scattering and radiative transfer theories (Liou, 2002). In this thesis, only optical methods are considered because the studied objects, aerosols, have the strongest impact on the electromagnetic radiation at these wavelengths. In optical remote sensing, despite the somewhat misleading name, ultraviolet, visible and infrared wavelengths are used, thus the available electromagnetic radiation spectrum for aerosol measurements ranges from circa 300 nm to circa 10 μm. These methods can be divided into four classes based on the location of the instruments and on the type of the instrument. The basic measurement concepts are shown in Figure 2.1. Ground-based instruments (A and B in Figure 2.1) are on the ground while spaceborne are aboard satellites (C and D in Figure 2.1). Passive instruments (A and C in Figure 2.1) measure radiation emitted by the sun and the Earth while active instruments (B and D in Figure 2.1) have their own radiation source, for example black body radiator or a laser. More detailed information on the measurement principles can be found in Chapter 3. These instruments can also be mounted onto airplanes. Although airborne measurements are widely used (e.g. Stone et al. (2010)), they are not discussed further in this thesis.

Unfortunately, not all the required radiative properties for aerosol studies can be measured remotely. For example, the angular and spectral ranges of remote sensing are always limited. Correspondingly, a core aspect of remote sensing is the inversion procedure, whereby aerosol optical and radiative properties are derived from the remote sensing measurements (Dubovik and King, 2000).

As can be seen from Figure 2.1, remote sensing instruments do not measure only aerosol signals. Clouds, atmospheric gases and the Earth's surface also affect the measured radiation signal and often their signal is larger than the aerosol signal. Therefore, the signals coming from these other sources have to be removed from the measured total signal before aerosol properties can be analyzed. The separation of the aerosol signal is done with inversion procedures.

There are several ways to do the inversion and all the methods have their strengths and weaknesses. Atmospheric gases absorb radiation at specific wavelengths, thus their measurement is quite straightforward and they can be taken into account in the retrieval quite easily. The surface, on the other, hand is more variable and the signal caused by it is relatively large at all wavelengths. Thus, separating aerosol signal from the surface signal is a demanding task. Therefore, aerosol retrievals from passive satellite measurements are more reliable over dark surfaces.

Inversion procedures for passive ground-based measurements are simpler because they do not have to take into account the surface effect. With active instruments, the measurement signal from the surface can be separated from the atmospheric signals based on the measurement time.

2.1 RADIATIVE TRANSFER

Remote sensing is based on the measurement of electromagnetic radiation, thus the understanding of radiative transfer in the atmosphere is essential when using data from these instruments. Radiative transfer is simply the physical phenomenon of energy transfer in the form of electromagnetic radiation. The propagation of radiation through a medium, which in our case is the atmosphere, is affected by absoption, emission and scattering processes. Radiative transfer theories and models describe these interactions mathematically. The main quantities associated with radiate transfer in the atmosphere and used in this work are introduced below.

Zenith angle, θ, measures the angle from some reference direction which in our case is the local vertical. Therefore, directly overhead corresponds to $\theta = 0$ and horizon to $\pi/2$ radians (90 degrees). *Azimuth angle*, ϕ, measures the angle counterclockwise from a reference point on the horizon, so that $0 < \phi < 2\pi$. In satellite applications, the reference point is usually the direction of the sun. Another important, although somewhat different, angle is the *solid angle* which is a measure of how much of your visual field is occupied by an object. It is expressed in units of steradian, sr (Petty, 2006).

Optical air mass, m, refers to the optical path length through the Earth's atmosphere. When the solar zenith angle is zero (sun directly overhead), the air mass factor is 1. The air mass factor increases as the solar zenith angle increases (Liou, 2002).

Flux (or more precisely flux density), F, refers to the rate at which radiation is incident on, or passes through a flat surface. It is expressed in units of watts per square meter and it includes energy contributions from all wavelengths between specified limits λ_1 and λ_2 (Petty, 2006).

Radiance (or radiant intensity), ρ, includes both the strength and direction of various sources contributing to the incident flux on a surface In other words, radiance is the flux per unit solid angle traveling in a particular direction [$\text{Wm}^{-2}\text{sr}-1$]. Within a vacuum or other transparent medium, radiance is conserved along any optical path (Petty, 2006).

Irradiance is the incident flux density, while *radiant exitance* is the exitent flux density. The ratio of these results in the so-called *reflectance*. The value of the reflectance is in the inclusive interval 0 to 1. This quantity can be further defined into more specific conceptual and measurable quantities. One of the most widely used quantities is the bihemispherical reflectance, commonly known as *albedo*, which is the ratio of the radiant flux reflected from a unit surface area into the whole hemisphere to the incident radiant flux of hemispherical angular extent. Another important quantity is the *bidirectional reflectance distribution function* (BRDF) which describes the scattering of parallel beam of incident radiation from one direction in the hemisphere into another direction in the hemisphere. Being expressed in as the ratio of infinitesimal quantities, it cannot be directly measured (Schaepman-Strub et al., 2006).

Transmission, T, is a term used when discussing the propagation of electromagnetic waves through a medium. *Transmittance*, τ, on the other hand, is the fraction of radiation that survives the trip over a specified optical path (Petty, 2006).

The rate of power attenuation per unit distance is given by the *extinction coefficient*, β_e, which is the sum of scattering (β_s) and absorbing (β_a) coefficients. The total *optical depth*, OD, (also known as optical thickness) can be calculated by integrating the extinction coefficients within a vertical column. Each (dimensionless) unit of optical depth corresponds to a reduction of intensity to $e^{-1} \approx 37$ % of its original value (Petty, 2006).

Index of refraction ($N = n_r + n_i$) within a nonabsorbing medium ($n_i = 0$) is the ratio of the speed of light in vacuum and the medium. For most materials, $N > 1$, which indicates a reduced speed of light relative to that in vacuum. When the imaginary part of the index is nonzero, the medium absorbs energy from the electromagnetic wave passing through. The relationship between the imaginary part (n_i) and absorption coefficient (β_a) is

$$\beta_a = \frac{4\pi n_i}{\lambda} \tag{2.1}$$

where λ is the wavelength in a vacuum. Index of refraction depends strongly on the wavelength of the radiation (Petty, 2006).

When the scattering is caused by small particles compared to the wavelength of the incident radiation, it is called *Rayleigh scattering*. It is also called molecular scattering because in the atmosphere these scatterers are typically molecules (gases). *Lorenz-Mie scattering*, on the other hand, refers to scattering by particles which are in the same size range as the wavelength of the radiation (Liou, 2002).

Scattering phase function, P_a, defined for a specific aerosol type tells how the incident radiation is scattered by these particles. It can be considered as a probability density: If a photon arrives from direction y and is scattered, what is the probability that its new direction will be x. The phase functions of real atmospheric particles can be complex and require sophisticated mathematical descriptions. Often, however, it is sufficient to know the relative proportion of photons that are scattered in the forward versus backward directions. This information is contained in the scattering *asymmetry parameter*, g (Petty, 2006).

Backscattering refers to radiation that is scattered back into the direction of the incident radiation beam (Petty, 2006).

The scattering of incident radiation by atmospheric molecules involves *elastic* and *inelastic* processes. In the case of elastic or Rayleigh scattering the wavelength of the scattered photon is the same as the wavelength of the incident photon. Thereby, the molecule preserves its vibration-rotation energy level during the scattering process. Inelastic or *Raman scattering* processes, on the other hand, lead to a change of the molecule's quantum state, and the wavelength of the scattered photon is shifted. If the molecule absorbs energy, the wavelength of the scattered photon is increased. This is called Stokes Raman scattering. If the molecule transfers energy to the scattered photon

by decreasing its energy level, the wavelength of the scattered photon is decreased. This is called anti-Stokes Raman scattering (Wandinger, 2005b).

A fundamental principle of electromagnetic radiation is that it at any instant of time displays some orientation in space. This orientation can be fixed, yielding linearly *polarized radiation*, or rotating with time to yield circularly or elliptically polarized radiation. Random polarization is a state in which a beam of radiation has such a diversity of individual wave polarizations that no single state can be discerned with optical analyzers. Importantly, any state of polarization can be converted to any other state with the help of optical devices (Sassen, 2005).

The basic polarization applications involve the transmission of a linearly polarized radiation pulse and the detection of the orthogonal and parallel planes of polarization of the backscattered radiation. The ratio of these two signals is referred to as the *linear depolarization ratio*, δ. According to the exact Lorenz-Mie theory, spherical particles that are homogeneous in content always backscatter linearly polarized electromagnetic radiation in the same (incident) plane of polarization. A variety of approximate theories predict that nonspherical or inhomogeneous particles will introduce a depolarized component in to the backscattering. The strength of the depolarization process in nonspherical particles depends on the amount and complexity of the particles' deviation from spherically symmetrical shape, but also on the particle size relative to the wavelength of the radiation and the particle refractive index at that wavelength. Consequently, little or no depolarization can be expected from spherical particles (e.g. deliquesced aerosols and volcanic sulfuric acid droplets) as long as they are reasonably homogeneous. For irregularly shaped particles (e.g volcanic and desert dust), the depolarization ratio can be up to 0.25 (Sassen, 2005).

Incident radiation can be divided into *diffuse* and *direct* components. Direct component refers to radiation that is coming directly from the source while diffuse radiation is scattered by the medium between the source and the sensor and the direction of the radiation coming to the sensor is from everywhere else but not directly from the source.

Figure 2.2 shows the main processes that can occur when radiation at different wavelengths interacts with particles. The radiation can be scattered at different directions or absorbed by the particles. The direction and amount of scattering (and absorption) depends on the wavelength of the radiation and on the size and chemical composition of the particles.

2.2   MEASURED AEROSOL PROPERTIES

Aerosols are defined as a mixture of solid and/or liquid particles suspended in a gas. (e.g. Hinds (1998)). The size (diameter) of the aerosol particles ranges from circa 2 nm to approximately 10 μm. Aerosols in the atmosphere have a number of sources. Typically the sources are divided into natural (e.g. wind blown dust, sea spray, volcanic ash and plant emissions) and anthropogenic (e.g. fuel combustion) sources (Seinfeld
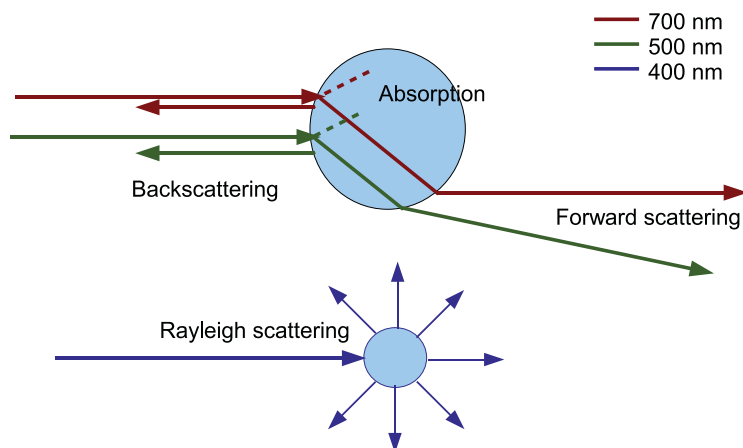
Figure 2.2. Interaction between incident radiation and particles.

and Pandis, 2006). Furthermore, the aerosols can be divided into primary and secondary aerosols. Primary aerosols are formed within a source and emitted directly into the atmosphere while secondary aerosols are formed in the atmosphere by gas-to-particle conversion (Fuzzi et al., 2006). The actual aerosol population in the atmosphere is a mixture of primary and secondary aerosols originating from natural and anthropogenic sources.

Aerosols are also important in air quality monitoring, where particulate matter (PM) describes the aerosol mass concentration. It can be further classified with size: $PM_{2.5}$ and PM_{10} contain aerosols with aerodynamic diameters less than 2.5 μm and 10 μm, respectively. Combustion processes are the most important source of $PM_{2.5}$. PM_{10} contains coarser components, for instance from natural sources (e.g. dust) elevated by wind (Pope and Dockery, 2006). A number of studies have been made where the usability of satellite measurements in air quality monitoring has been evaluated (e.g Christopher and Gupta (2010); Sano et al. (2010); Weber et al. (2010)). Since PM describes mass concentration and parameters from satellite measurements are optical quantities, it is not straightforward to compare them directly. Furthermore, the methods for the measurements are completely different. PM is a ground-based point measurement whereas satellite based aerosol properties are derived from remotely sensed radiance signals, which cover relatively large areas.

In remote sensing the retrieved aerosol parameters are a bit different than the traditional parameters (e.g. aerosol number concentrations, size distributions, mass, scattering and absorption coefficients) from in-situ measurements. The most widely used aerosol properties derived from remote sensing measurements are:

- aerosol optical depth (AOD) which is a measure of how much light airborne particles prevent from passing through a column of atmosphere. It describes the total aerosol extinction (scattering + absorption, Figure 2.2) (Liou, 2002).

- Ångström Exponent (AE) describes the dependency of AOD (or extinction) on wavelength. AE can be calculated from spectral AOD data using the Ångström's power law (Ångström, 1929):

$$AE = -\frac{log(\frac{AOD_1}{AOD_2})}{log(\frac{\lambda_1}{\lambda_2})} \qquad (2.2)$$

The smaller the particles are, the larger is the exponent. Typically values larger than 1 are associated with fine dominated aerosols (e.g. smoke, sulphates) while the values smaller than 1 indicate the presence of coarse particles (e.g. dust, marine aerosols) (Eck et al. (1999); Schuster et al. (2006)).

- Single Scattering Albedo (SSA) is the ratio of scattering to total extinction. The smaller the ratio, the more the aerosols absorb (Liou, 2002).

Effects of atmospheric aerosols on radiative transfer are complex to model, as discussed in Paper I, because aerosol size distributions vary strongly both temporally and spatially. Moreover, the optical properties of atmospheric aerosols are not fully known (Bond and Bergstrom, 2006). Patchy sources, sinks, and the short atmospheric lifetime (days) of tropospheric aerosols result in local effects and regional differences in aerosol properties (Delene and Ogren, 2002). According to Anderson et al. (2003) aerosol concentrations are typically coherent for timescales and space scales less than 10 h and 200 km, respectively. Algorithms used in retrieving satellite data assume that aerosol properties are constant and therefore the actual variability in aerosol optical properties can cause uncertainties in satellite-retrieved parameters.

In this work, the term aerosol model refers to assumed aerosol size distributions and optical properties (e.g. phase function and SSA) used in radiative transfer calculations.

3 OPTICAL REMOTE SENSING INSTRUMENTS

3.1 GROUND-BASED

3.1.1 Passive

The most widely used remote sensing instruments in aerosol studies are radiometers, historically known as sun photometers (instrument A in Figure 2.1). The method for ground-based atmospheric aerosol measurements using sun photometry was introduced by Volz in the end of 1950's (Volz et al., 1959). The first sun photometer was a handheld analog instrument. Nowadays, the instruments are digital with onboard processing and automatic data transfer. However, the measurement method has remained the same; a filtered detector measures the spectral extinction of direct beam radiation according to the Beer-Lambert-Bouguer law:

$$V_\lambda = V_{0\lambda} d^2 exp(OD_\lambda m) \times T_y \qquad (3.1)$$

where V = digital voltage,

V_0 = extraterrestrial voltage

d = ratio of the average to the actual Earth-Sun distance

OD_λ = total optical depth

m = optical air mass

T_y = transmission of absorbing gases

The measured voltage (V) at a specific wavelength (λ) is a function of the extraterrestrial voltage (V_0) as modified by the relative Earth-Sun distance (d), and the exponent of the total optical depth (OD_λ) and optical air mass (m). The total optical depth is the sum of the Rayleigh and aerosol optical depth (AOD) after correction for gaseous absorption (Holben et al., 1998).

Basic sun photometers, e.g. Precision Filter Radiometers (PFR), measure only spectral OD. Sky scanning spectral radiometers, e.g. Cimel sun photometers, are more sophisticated and measure the spectral sky radiance at known angular distances from the Sun. With an inversion algorithm, aerosol microphysical properties such as size distribution and optical properties such as phase function, can be retrieved from these measurements (Holben et al., 1998). The inversion algorithm is designed as a search for the best fit of all input data by a theoretical model that takes into account the different levels of accuracy of the fitted data (Dubovik and King, 2000).

In addition to sun photometry, AOD can be derived from other instruments. For example, rotating shadowband radiometers measure spectral total and diffuse radiation to obtain the direct component from which the AOD can be calculated with the Equation 3.1 (Holben et al., 1998). Moreover, aerosol measurements can be done with Differential Optical Absorption Spectroscopy (DOAS) which was developed for the measurement of atmospheric constituents. The amount of the constituents can be retrieved from the measurements of direct solar radiation transmitted through the atmo-

sphere as well as of the solar radiation scattered in the atmosphere or reflected from the surface (Rozanov and Rozanov, 2010). The key constituents monitored with this instrument are ozone (O_3), nitrogen dioxide (NO_2), formaldehyde (HCHO), the halogen oxides (e.g. BrO), Chlorine dioxide (OClO), iodine monoxide (IO), and the oxygen diomer (O_4). Information about the atmospheric aerosol profile can be retrieved from the O_4 measurements (Whyte et al., 2009). In addition, Multi-Axis-DOAS (MAX-DOAS) provides information on the aerosols based on the Ring effect. The Ring effect describes the so-called "filling-in" of solar Frauenhofer lines in the spectra of scattered light compared to direct sun light observations. The effect is caused by the rotational Raman scattering by atmospheric molecules and aerosols (Wagner et al., 2009).

In Paper II we used Precision Filter Radiometer (PFR) measurements (Wehrli (2000); Kim et al. (2008a). PFR measures direct solar irradiance in four narrow spectral bands (368, 412, 500, and 862 nm). The bandwidth of the instrument is 5 nm and the full field of view angle is 2.5 degrees. Derived products from the measurements are AOD for the four wavelengths and AE. The time resolution of the products is 1 minute. The uncertainty of the PFR instrument is between 0.01 and 0.02 (Carlund et al., 2003).

In Papers II, III, IV we used data from Cimel sun photometer measurements. Cimel is the instrument selected for the Aerosol Monitoring Network (AERONET; Holben et al. (1998)), which has almost a global coverage. Cimels measure AOD at 340, 380, 440, 500, 675, 870 and 1020 nm. Measurements are provided every 15 minutes during daytime. Once every hour in clear sky conditions AERONET also provides the angular distribution of sky radiances at four wavelengths (440, 670, 870 and 1020 nm), from which aerosol properties such as aerosol size distribution, complex refractive index, and SSA can be retrieved. The spectral AOD from AERONET are accurate to within ± 0.01 for wavelengths larger than 400 nm and ± 0.02 for shorter wavelengths (Holben et al. (1998); Eck et al. (1999)).

3.1.2 Active

In contrast to passive remote sensing methods, active instruments have their own radiation source. Depending on the wavelength(s) of the radiation emitted by the source, the instrument can be used to study different atmospheric phenomena.

Transmissometers are instruments designed to measure the atmospheric extinction coefficient and determine visibility. The instrument has typically a blackbody radiation source or a laser, which transmits a beam of optical radiation into the atmosphere. The beam is attenuated by scattering and absorption in molecules and aerosol particles. After a designated distance, the signal is measured with a detector. The extinction coefficient can be calculated based on the amount of attenuation in the signal and the propagation length in the atmosphere (Hågård and Persson, 1992). Visibility and atmospheric extinction can also be measured with scatterometers. These instruments measure the amount of light scattered by aerosols in an optical volume, observed within

a small solid angle. The extinction coefficient can be derived on the basis of the light scattering functions of aerosols (van der Meulen, 1992).

A more sophisticated active instrument is the lidar (light detection and ranging; instrument B in Figure 2.1). The history of lidars begins in the 1930's when first attempts to measure air density profiles were done with searchlight beams. In 1938, cloud base heights were measured for the first time with pulses of light. In these early years, electric sparks and flashlights were used as light sources. In the beginning of the 1960's the laser was invented and it enabled the development of modern lidar technologies. Already in the 1970's, all basic lidar techniques had been suggested and demonstrated (Wandinger, 2005a).

Just like the transmissometers, a lidar consists of transmitter and a receiver. The laser generates short light pulses with lengths of a few to several nanoseconds at specific wavelengths. The light pulses go through a beam expander before entering the atmosphere, in order to reduce the divergence of the light pulses. The receiver has a telescope that collects the photons backscattered from the atmosphere. After the telescope, the photons enter an optical analyzing system which selects specific wavelengths out of the collected light. Then the selected radiation is directed onto a detector, where the photons are transformed into an electrical signal. The intensity of the signal and its dependence on the time elapsed after the transmission of the light pulse are determined electronically and stored (Wandinger, 2005a).

The detected lidar signal can simply be written as

$$P(R) = KG(R)\beta(R)T(R) \tag{3.2}$$

where P is the power received from a distance R. It consists of four factors. The first factor, K, summarizes the performance of the lidar system, while the second, $G(R)$, describes the range-dependent measurement geometry. These two factors depend only on the lidar setup. The last two factors contain the information on the atmosphere, and all the measurable quantities. The factor $\beta(R)$ is the backscatter coefficient at distance R and $T(R)$ is the transmission term. This simplified equation shows the basic principle of lidar measurement. However, for actual measurements the lidar equation has to be more detailed:

$$P(R, \lambda) = P_0 \frac{ct}{2} A\nu \frac{O(R)}{R^2} \beta(R, \lambda) exp[-2S_0^R \alpha(r, \lambda) dr] \tag{3.3}$$

where P_0 is the average power of a single laser pulse, t is the temporal pulse length and, consequently, ct is the length of the volume illuminated by the laser pulse at a fixed time. The term is divided by 2 because of an apparent "folding" of the laser pulse through the backscatter process. A is the area of the primary receiver optics and ν is the overall system efficiency. These five parameters correspond to the term K in Equation 3.2. The term $O(R)$ describes the laser-beam receiver field-of-view overlap function and with R^2 they are included in the term $G(R)$ of Equation 3.2. The term $\beta(R, \lambda)$ describes the backscatter of the laser light caused by air molecules

and particulate matter at wavelength λ. The final part of the lidar equation ($T(R)$ in Equation 3.2) takes into account the fraction of light that gets lost on the way from the lidar to the scattering volume and back. This exponental term comes from the specific form of the Lambert-Beer-Bouguer law for lidars and it can have values between 0 and 1. The integral contains the path from the lidar to distance R and due to the two-way transmission it is multiplied by 2. The sum of all transmission losses is referred as light extinction, and $\alpha(R, \lambda)$ is called the extinction coefficient (Wandinger, 2005a).

At the moment, there are some networks for lidars. For example, EARLINET (A European Aerosol Research Lidar Network to Establish an Aerosol Climatology) (Wiegner et al., 1999) has 27 ground-based lidars, but only in Europe. Another widely recognized lidar network is the Micropulse Lidar network (MPLNET) (Welton et al., 2001), which has 31 sites collocated with AERONET sun photometers around the globe.

In Paper I we made continuous aerosol attenuation measurements with an modernized OLAF-transmissometer which was constructed by Swedish Defence Research Agency (Hågård and Persson, 1992). The OLAF-transmissometer measures attenuation of infrared radiation in three bands: 0.96-1.08 μm, 3.4-4.3 μm and 7.7-16.5 μm. It includes a transmitter-receiver unit, a reflector, control electronics and a computer. A measurement beam through the atmosphere and a reference beam inside the device are generated from a 1500 K Globar radiation source. The measurement beam travels 495 m to the reflector and back, thus the total path length in the atmosphere is 990 m. The path distance to the ground varies between 2 to 5 meters. By comparing electronically the detected power values of these two beams, the value for the attenuation in the atmosphere can be determined. Since OLAF measures the total attenuation in the atmosphere, the attenuation caused by aerosols is obtained by subtracting the part caused by atmospheric gases. Only carbon dioxide and water vapor have a significant impact on the radiative transfer at the OLAF wavelength bands. The effect of these gases is calculated with a radiative transfer code (MODTRAN4). The extinction coefficient β_e can be estimated from the transmittance τ according to Beer-Lambert's equation

$$\tau = e^{-\beta_e L} \tag{3.4}$$

where L is the path length of the radiation in the atmosphere.

OLAF's relative error has a parabolic dependence on measured extinction coefficient in all wavelength bands. For the longest wavelength band (7.7–16.5 μm) the relative error is less than 10 % when the measured extinction coefficient is between 0.23-3.5 km^{-1}. When the measured extinction coefficient is between 0.11-0.23 km^{-1} or between 3.5-4.4 km^{-1} the relative error is less than 20 %. The accuracy of the OLAF-transmissometer is confined especially by Globar's quite low radiant exitance as wavelength increases, by the noise in the pyroelectric detector and by the deviation of the system transmission (Kaurila et al., 2006).

In Paper V, we made measurements with a seven-channel Raman lidar called

"Polly^{XT}-POrtabLe Lidar sYstem eXTended" (Althausen et al., 2009). The lidar system is completely remotely controlled and all measurements and data transfer are performed automatically. The instrument is equipped with an uninterruptible power supply (UPS) and an air conditioning system (A/C) to allow a safe and smooth continuous measurements. A rain sensor is connected to the roof cover to assure a proper shutdown of the instrument during rain. In addition the system is equipped with an airplane radar, which shuts down the laser in case an airplane is detected.

The type of the laser used in the lidar is Inlite III from Continuum. It emits energy simultaneously approximately 180 mJ, 110 mJ, and 60 mJ at 1064 nm, 532 nm, and 355 nm, respectively. The emitted radiation is linearly polarized at 355 nm. A beam expander is used to enlarge the beam from approximately 6 mm to about 45 mm before it enters the atmosphere. The backscattered signal is collected by a Newtonian telescope which has a main mirror with a diameter of 300 mm and a focal length of 900 mm. The receiver's field of view is 1 mrad.

The output of the instrument includes vertical profiles of the particle backscattering coefficient at three wavelengths (355, 532 and 1064 nm) and of the particle extinction coefficient at two wavelengths (355 and 532 nm). AOD can be calculated by vertically integrating the extinction coefficient profile. In addition, such size/composition-dependent, intensive particle quantities as the AEs for backscatter and extinction, extinction-to-backscatter ratio and depolarization ratio can be determined. The depolarization channel (355 nm) of the lidar enables us to separate spherical particles from non-spherical and hence ice-containing from water clouds. In addition, dust and ash aerosols can be separated from other aerosol types. The vertical resolution of the system is 30 meters. Depending on the cloudiness, the whole troposphere can be monitored.

3.2   SPACEBORNE

The history of satellites began in 1957 when the Russians launched Sputnik 1 into an Earth orbit. Only four months later, the Americans launched their first satellite, Explorer 1, which was the first satellite to carry scientific instrumentation. The first visual observations of the atmospheric aerosols were made from manned spacecrafts. In 1961, cosmonaut Yuri Gagarin observed clouds and optical phenomena due to the presence of aerosols during the first manned space flight. In the following space flights photography was used to study the vertical distribution of aerosols. In the 1970's astronauts/cosmonauts made aerosol measurements with spectrophotometers and sun photometers. The first aerosol measurements from an un-manned spacecraft were also made in the end of the 1970's. These instruments, although not solely designed for aerosol measurements, started the era of satellite-based aerosol remote sensing (Lee et al., 2009).

Spaceborne instruments have the same measurement principles as the ground-based devices. However, the measurement environment is much more demanding. The

instrument design has to be robust to survive the launch to space and to be able to operate years without proper maintenance.

3.2.1 Passive

Retrieving aerosol properties over land and ocean is a very complex task for passive optical satellite techniques. The observed signal at the satellite level is a combination of surface and atmospheric contributions (see Figure 2.1, instrument C). In addition, the aerosol contribution has to be separated from the atmospheric signal (molecular and cloud scattering). Typically the surface signal is substantially larger than the aerosol contribution, especially over land. The most challenging surfaces are deserts and snow due to their high reflectivity. Moreover, clouds prevent the measurement of aerosols entirely (Kokhanovsky et al., 2007).

At the time of writing the thesis, a wide range of passive instruments used for aerosol retrievals are orbiting the Earth. The most widely used instruments are: AATSR (Grey et al. (2006); Thomas et al. (2009)), MERIS (Santer et al. (1999);Santer et al. (2000); von Hoyningen-Huene et al. (2003)), MISR (Kahn et al. (2001); Diner et al. (2005); Keller et al. (2007)), MODIS (Levy et al. (2007); Remer et al. (2005); Hsu et al. (2006); Lee et al. (2006)), OMI (Torres et al., 2007), POLDER (Deuze et al. (2001); Dubovik and King (2010)), and SCIAMACHY (Di Nicolantonio et al., 2006). Furthermore, measurements done with a single instrument can be processed with a number of different retrieval algorithms. However, due to the diversity of the algorithms and approaches, the aerosol properties for a specific ground pixel from these instruments are not always consistent with each other. The issue is further complicated by the fact that the information content of the aerosol measurement done with a satellite instruments is underconstrained. Usually, it is not possible to constrain the phase function and the SSA of the aerosols from the measurements themselves. Therefore, *a-priori* assumptions based on prescribed aerosol models are used. Depending on the accuracy of the aerosol properties assumed, and the performance of the algorithms, different values of AOD may be retrieved for the same measurement (Kokhanovsky et al. (2007); Kokhanovsky et al. (2010)).

In Papers II and IV we used data from the Moderate Resolution Imaging Spectroradiometers (MODIS; Salomonson et al. (1989)). These instruments are aboard the Terra and Aqua satellites. Terra MODIS and Aqua MODIS cover the Earth's surface every 1 to 2 days. These instruments have 36 spectral bands and they measure near-nadir (directly below the instrument) radiance over a 2300-km wide swath. The resolution of the measurements varies between 0.25 to 1 km (Anderson et al., 2005). By aggregating the finer resolution pixels, MODIS can separate cloudy and clear sky pixels so that there is enough signal to consistently and accurately retrieve aerosol properties on 10 km x 10 km resolution (Levy et al., 2007). Remote sensing of aerosols with MODIS is based on the relationship between the measured radiance at the top of the atmosphere

ρ^* and the surface bidirectional reflectance properties $\rho(\theta, \theta_0, \phi)$:

$$\rho^*(\theta, \theta_0, \phi) = \rho_a(\theta, \theta_0, \phi) + F_d(\theta_0)T(\theta)\rho(\theta, \theta_0, \phi)/(1 - s\rho^{'}) \qquad (3.5)$$

where θ is the view zenith angle, θ_0 is the solar zenith angle and ϕ is the azimuth angle of the scattered radiation from the solar beam; $\rho_a(\theta, \theta_0, \phi)$ is the path radiance, and $F_d(\theta_0)$ is the normalized downward flux for zero surface reflectance, equivalent to the total downward transmission. $T(\theta)$ is the upward total transmission into the satellite field of view, s is the atmospheric backscattering ratio and ρ' is the angular spectral surface reflectance (Kaufman et al., 1997). The path radiance (ρ_a) is proportional to the AOD, the aerosol scattering phase function $P_a(\theta, \theta_0, \phi)$ and SSA:

$$\rho_a(\theta, \theta_0, \phi) = \rho_m(\theta, \theta_0, \phi) + SSA * AOD * P_a(\theta, \theta_0, \phi)/(4\mu\mu_0) \qquad (3.6)$$

where $\rho_m(\theta, \theta_0, \phi)$ is the path radiance due to molecular scattering, μ and μ_0 are cosines of the view and illumination directions, respectively. The functions F_d, T and s are also dependent on aerosol type and loading (SSA, AOD, $P_a(\theta, \theta_0, \phi)$). However, for small surface reflectance they are less important (Kaufman et al., 1997). The Equation 3.6 is valid for single scattering approximation of aerosols and it does not include interaction of aerosols with molecules and surface. Therefore, it can only be applied when AOD, Rayleigh scattering and surface reflectance are low. For situations with high AOD and high Rayleigh scattering multiple scattering needs to be considered.

The MODIS second-generation operational algorithm performs a simultaneous inversion of two visible (0.47 and 0.66 μm) and one shortwave-IR (2.12 μm) channel, making use of the coarse aerosol information content contained in the 2.12 μm channel (Levy et al., 2007). The expected error over land in the MODIS AOD is $\pm 0.05 \pm 0.15$*AOD. This total uncertainty includes the uncertainties in assumed aerosol and land surface optical properties, radiative transfer computations, as well as, issues of cloud masking, pixel selection, instrument calibration and precision (Levy, 2009). Levy et al. (2010) reported that the only accurate aerosol parameter in the current retrieval is AOD. Other parameters, e.g. AE, can have unphysical values.

3.2.2 Active

Currently, there is only one active remote sensing instrument designed for the measurement of aerosols (instrument D in Figure 2.1) on the orbit . The Cloud-Aerosol Lidar and Infrared Pathfinder Satellite Observation (CALIPSO) satellite (Winker et al. (2003); Vaughan et al. (2004)) was launched successfully in April 2006, and measurement data has been available from June 2006 onward. CALIPSO carries the Cloud-Aerosol Lidar with Orthogonal Polarization (CALIOP) instrument, which can measure the vertical structure of the atmosphere at three channels, from the intensity of that part of the (pulsed) laser light that is scattered back to the lidar receiver. Two of these channels, at 532 nm, are orthogonally polarized and one channel measures the total

backscattered signal at 1064 nm. The diameter of the laser pulse at ground level is about 70 m. CALIOP has a spatial resolution of 333 m along the orbital path and a high vertical resolution (30-60 m). The satellite repeat cycle is 16 days (Winker et al., 2007). Due to the small footprint, CALIPSO covers only 0.2 % of the Earth's surface during one repeat cycle (Kahn et al., 2008). CALIOP delivers important information on the vertical structure of the atmosphere globally. This information is complementary to ground-based lidars which provide detailed time-series representative for specific locations.

CALIOP is an elastic backscatter lidar which can not measure extinction in the atmosphere. Therefore, both the particulate backscatter coefficient and particulate extinction coefficient at a given range are unknown variables. They have to be retrieved with a single equation, thus the retrieval is underdetermined. However, the two unknowns can be related to each other by the aerosol extinction-to-backscatter ratio, which is commonly known as the *lidar ratio*, S_a. The lidar ratio has to be either assumed or inferred from additional measurements in order to solve the lidar equation (Klett, 1981). The actual value of the aerosol lidar ratio depends on three parameters: particle composition, size distribution, and morphology. Consequently, the variation in the ratio is large ($10 < S_a < 110$) (e.g., Ferrare et al. (2001)). The operational CALIOP algorithm must infer a value of S_a for each aerosol layer in order to retrieve aerosol backscatter and extinction coefficients from the measurements. The goal of the CALIOP algorithm is to define S_a to within 30 % (Omar et al., 2009). This requirement can often be reached without complete knowledge of the aerosol type. However, error in the assumed value of S_a creates errors in both the backscatter and extinction profiles (Sasano et al. (1985); Fernald et al. (1984)). In CALIOP processing, furthermore, errors due to incorrect lidar ratios propagate downward as the attenuation by upper layers is corrected in the retrieval of lower layers (Young and Vaughan (2009); Winker et al. (2009)), thus errors are of particular concern for near-surface applications, e.g. air quality studies (Burton et al., 2010). Moreover, the operational CALIOP algorithm assigns the S_a for each aerosol layer based on the inferred aerosol type of the layer. If the aerosol typing of the layer fails, so will the more sophisticated parameters, e.g. AOD. Therefore, the quality of this aerosol typing was evaluated in Paper IV

The basic characteristics of all the discussed remote sensing methods are summarized in Table 3.1.

Table 3.1 Remote sensing methods: basic characteristics. + signs indicate the advantages of
the methods, while - signs refer to the disadvantages.

	Ground based	Spaceborne
PASSIVE	● measures direct and diffuse radiation from the sun ● point measurement + no surface effects - clouds prevent measurements	● measures radiation reflected and emitted by the Earth-Atmosphere system ● areal average + global data from a single instrument - clouds, ice and snow prevent measurements
ACTIVE	● measures radiation emitted by instrument's own source ● temporal average + vertical profile + clouds and aerosols with a single measurement - scarce network	● measures radiation emitted by instrument's own source ● areal average + vertical profile + clouds and aerosols with a single measurement - narrow swath

4 MAIN RESULTS

4.1 EVALUATION OF THE DERIVED AEROSOL PRODUCTS

In order to to evaluate the quality of the aerosol products derived from optical remote sensing measurements, we studied different methods and compared the retrieved parameters with results from other instruments. Typically, AERONET measurements were used as a "ground truth" due to their robust and extensively quality controlled data products.

The fundamental difficulty in remote sensing is discussed in Paper I where measured and modeled aerosol extinction coefficients were studied as a function of different weather parameters (visibility, relative humidity and temperature). These ground-based measurements were done in Lakiala, Finland. In addition, measured size distributions were investigated and compared with the size distribution assumed in MODTRAN4 radiative transfer model. MODTRAN4 has several default size distributions from which the rural distribution was found most suitable for the area under study. Clear differences between the measured size distributions and model size distribution were found. The measurements indicated 2200 particles per cm^3 on average for the studied weather conditions, while the model distribution assumed 13289 particles per cm^3. Moreover, there was no clear relationship between the measured attenuation values and the weather parameters (relative humidity, visibility and temperature), thus weather parameters do not offer the most feasible input data to model the aerosol extinction. In addition, the errors in weather parameter measurements can cause a cumulative error up to 130 % in the calculated aerosol extinction in the worst case. Finally, aerosol extinction coefficients calculated from the measured size distributions were much lower than the values measured with OLAF transmissometer or modeled with MODTRAN4. This indicates that the assumed optical properties (e.g. refractive index) and growth factors (ratio of the aerosol diameter at ambient relative humidity to the diameter at dry air) of the aerosols were not suitable for the location under study. This underlines the fact that in order to transform microphysical properties (size distribution, chemical composition and particle shape) into optical properties (spectral extinction, aerosol phase function and SSA) some assumptions have to be made. By utilizing Mie theory in the calculation of light scattering we assume that the particles are spherical which is not valid for all aerosol types. Furthermore, we have to assume how the particle size varies with relative humidity because we do not know how much moisture the particles absorb from the air due to our limited knowledge of their chemical composition. Therefore, the use of aerosol models based on microphysical properties can lead to uncertainties in radiative transfer calculations.

As a next step, we evaluated the performance of an operational satellite algorithm designed for aerosol retrieval. In paper II, AOD and AE values derived with the MODIS retrieval algorithm over land (Collection 5) were compared with ground based sun photometer measurements in Europe, Asia, Africa North America and South America. In

Finland (Jokioinen and Sodankylä) the measurements were done with Precision Filter Radiometers (PFR), while in Estonia (Tõravere), Italy (Ispra, Rome Tor Vergata), India (Kanpur), China (Xianghe), USA (GSFC, Greenbelt), Mexico (Mexico City), Zambia (Mongu) and Brazil (Alta Floresta) Cimel (AERONET) measurements were used. Comparison results for AOD were generally good, although there seems to be room for improvement in the MODIS aerosol model selection, particularly how dust is taken into account. At all studied sites, the MODIS algorithm often selects the dust aerosol model even when dust does not seem to be present and the air masses are not coming from arid regions. This happens especially when AOD values are relatively small ($<$ 0.3). The selection of the dust model reduces the correlation between ground based and MODIS AOD measurements in dust-free situations. Moreover, the current aerosol model selection scheme produces unphysical AE values (Levy et al., 2010).

To evaluate the quality of the aerosol measurement done with a spaceborne lidar, we compared the aerosol subtypes of CALIOP measurements with daily aerosol types derived from AERONET level 2.0 inversion data, as presented in Paper III. AERONET aerosol types were categorized by SSA and AE values. The comparison showed that 70 % of the CALIOP and AERONET aerosol types were in agreement. Best agreement was achieved near desert regions for dust and polluted dust types. In the areas influenced by fine aerosols the level is lower, about 57 %. Classification of dust is more reliable than classification of fine aerosols because depolarization ratio can be used to distinguish non-spherical aerosols from spherical ones. The quality of the aerosol type classification is extremely important because aerosol properties assigned for the layers depend on the selected types.

4.2 IMPROVEMENTS FOR AEROSOL REMOTE SENSING METHODS

Retrieval of aerosol properties from optical remote sensing measurements is typically underdetermined and some a-priori assumptions are required. Usually, these assumptions concern aerosol models (size distribution, SSA, g) and surface properties. As Paper I showed, for accurate aerosol extinction modeling, the assumed aerosol size distributions, refractive indices and growth factors have to coincide with the reality.

In Paper II, our study suggested that the aerosol model combining in the retrieval algorithm is sensitive to the ratio of 660 nm and 2130 nm surface reflectances (slope(660/2130)). Furthermore, the value of the slope used is mainly dependent on the Normalized Difference Vegetation Index (NDVI). NDVI describes the "greenness" of vegetation and it can be used for determining the surface type. Usually, it is defined as a function of the red and near-infrared radiation. In this work, however, NDVI is defined as

$$NDVI = \frac{\rho_{1.24} - \rho_{2.12}}{\rho_{1.24} + \rho_{2.12}} \tag{4.1}$$

where $\rho_{1.24}$ and $\rho_{2.12}$ are measured reflectances at the top of the atmosphere (Levy et al., 2007).

Figure 4.1. Dependence of slope(660/2130) on NDVI for forest ecotypes based on MODIS surface albedo data. The solid black line indicates the relationship of the parameters used in the MODIS retrieval while the dashed line is the inverse version of it.

Figure 4.2. Dependence of slope(660/2130) on NDVI for savanna ecotypes based on MODIS surface albedo data. The solid black line indicates the relationship of the parameters used in the MODIS retrieval while the dashed line is the inverse version of it.
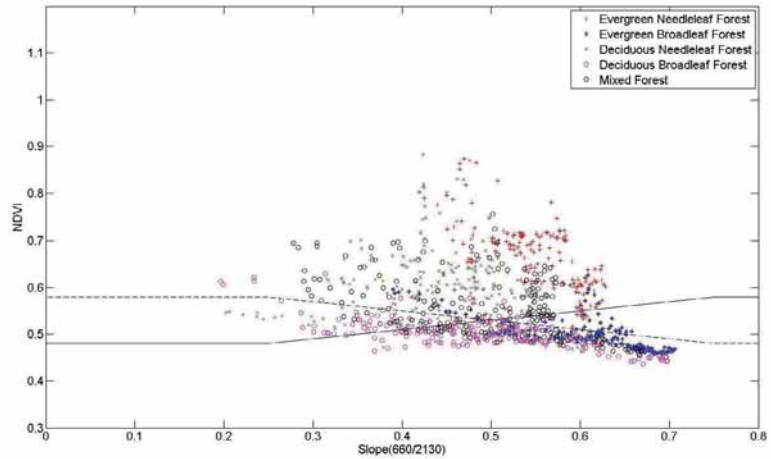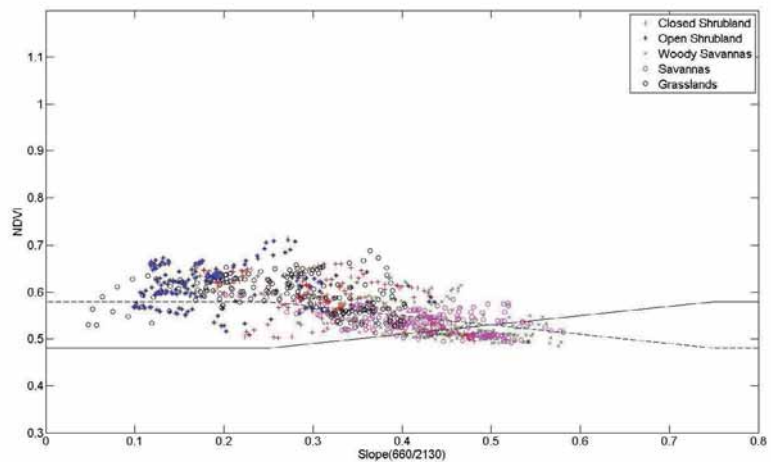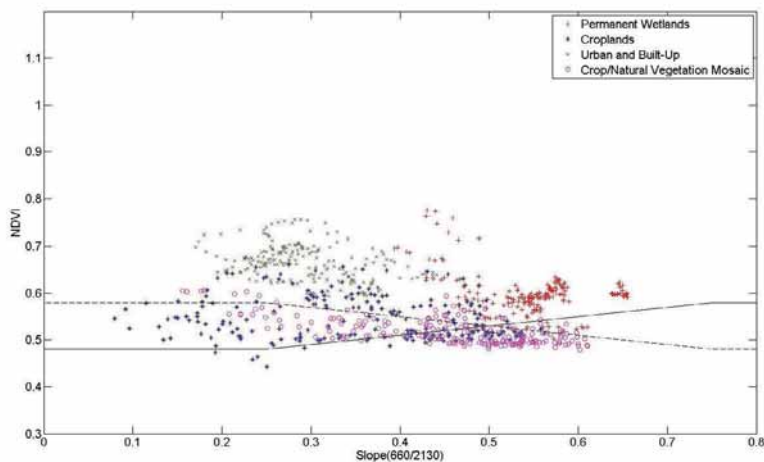
Figure 4.3. Dependence of slope(660/2130) on NDVI for different ecotypes based on MODIS surface albedo data. The solid black line indicates the relationship of the parameters used in the MODIS retrieval while the dashed line is the inverse version of it.

The current relationship of the slope and NDVI in the algorithm is not supported by the surface albedo climatology derived from MODIS surface measurements. In addition, the albedo data show that the slope-NDVI relationship depends strongly on the underlying ecotype, as can be seen from Figures 4.1- 4.3. The use of a more physical relationship improves the AE retrieval at the studied sites (Alta Floresta, Kanpur, Mexico City, Mongu, Rome, and Xianghe). However, at some sites (e.g. Mongu and Xianghe) the AOD correspondence deteriorates when the new relationship is used. Nonetheless, the possibility to take this into account in the future MODIS aerosol retrievals should be studied further. In addition, AOD retrievals could be improved at some of the studied sites (e.g. Alta Floresta and Mongu) by changing the assigned fine dominated aerosol model.

During the research presented in Paper III we assessed whether the CALIOP classification scheme for aerosol subtypes could be improved by adding color ratio data (the ratio of the layer-integrated attenuated backscatter at 1064 nm by the layer-integrated attenuated backscatter at 532 nm) to the scheme in order to give additional information on the size of the aerosols in a similar manner as AE. While AE is based on measurements of total attenuation (scattering and absorption) of radiation, color ratio is based on backscattering. In order to compare as similar parameters as possible, we calculated the scattering induced AOD from the AERONET inversion data by reducing the absorption induced AOD from the total AOD at two wavelengths, 440 nm and 1020 nm. Then, we compared the ratio of the scattering AODs ($AODScat_{1020}/AODScat_{440}$) to the color ratios for the comparison days. In addition, we checked if the instruments
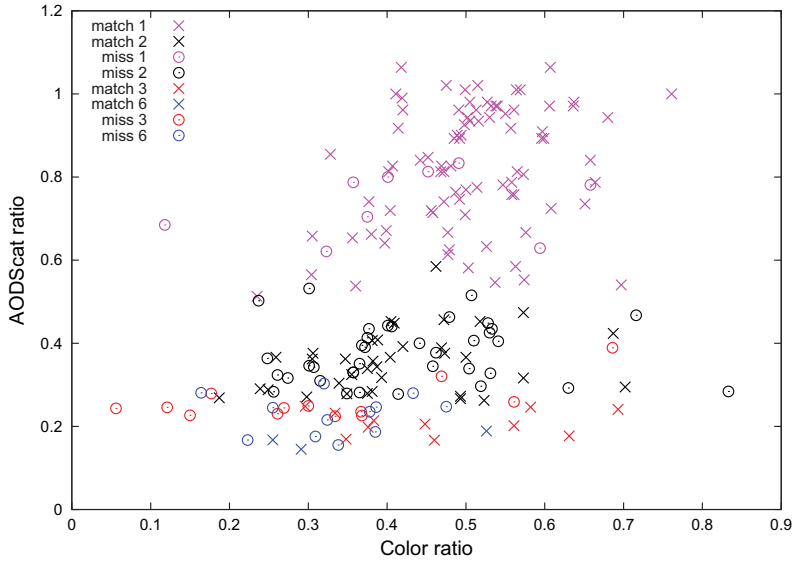
Figure 4.4. Comparison of color ratio from CALIOP and ratio of scattering AOD at 1020 nm and 440 nm (AODScat ratio) from AERONET for different aerosol types. Aerosol types 1 (Large absorbing, magenta), 2 (Mixed absorbing, black), 3 (Small absorbing, red) and 6 (Small non-absorbing, blue) are shown. Crosses refer to measurements where CALIOP and AERONET aerosol types agree (match) and circles where they disagree (miss).

had agreed on the aerosol type for that day. Figure 4.4 shows the daily mean AODScat ratio and color ratio values for different aerosol types. The color of the point indicates the aerosol type of the measurement. Crosses refer to measurements where CALIOP and AERONET aerosol types agree (match) and circles where they disagree (miss). Although color ratio correlates to some extent with AODScat ratio (R = 0.59), the variation of the parameter is large for each aerosol type and the values are all in the same range. Moreover, the matched and missed measurements are mixed evenly. Thus, color ratio does not seem to introduce additional information about the aerosol types to the classification scheme. In addition, the largest difficulties in the CALIOP aerosol typing occur with small aerosols. CALIOP is not able to distinguish absorbing aerosols from non-absorbing because it has no measurements on the absorptivity of the aerosols.

4.3   APPLICATIONS OF REMOTE SENSING MEASUREMENTS

As discussed in the previous sections, remote sensing of the atmospheric aerosols is not a trivial task. A number of assumptions have to be made before aerosol retrieval is feasible. However, some of the current remote sensing products are robust enough for

more extensive analysis.

Despite the difficulties in the AE retrieval with the MODIS aerosol algorithm (discussed in section 4.1 and Paper II), the AOD product is substantially more reliable. Thus, it can be used for air quality studies as shown in Paper IV, where the relationship between satellite-based AOD and particulate matter ($PM_{2.5}$) was studied. $PM_{2.5}$ was measured at four sites (Kallio, Mannerheimintie, Vallila and Luukki) near each other within Helsinki region, Finland. We investigated how temporal $PM_{2.5}$ averaging affected the correlation between $PM_{2.5}$ and AOD. In addition, we studied the seasonality of the correlation. The time averaging increased the correlation coefficient compared to one-hour $PM_{2.5}$ measurements. The best correlation coefficients were achieved with 5 to 24 h averaging, depending on the site. In Luukki, the largest correlation coefficient was 0.82 with 24 h averaging, while in Vallila the largest correlation coefficient was only 0.55 with 5 h averaging. Regarding the monthly averages of $PM_{2.5}$ and AOD, the correlation coefficients were between 0.57 and 0.91, slightly better than the best temporal average at each site. We also studied $PM_{2.5}$ and AOD gradients between an urban and a rural site. Monthly averages at the urban site were regularly higher than those at the rural site. However, the seasonal behavior was similar. Moreover, we studied the urban influence on AOD-PM association. This analysis resulted in better correlation at the rural site (0.87) than for the averaged urban data (0.73). The slopes of our $PM_{2.5}$ and AOD relationships were between 0.013 $\mu mg^{-1}m^3$ and 0.017 $\mu mg^{-1}m^3$, which are in agreement with other studies. Based on these results, long-term $PM_{2.5}$ can be estimated from AOD data for the Helsinki region. Furthermore, the correspondence between $PM_{2.5}$ and AOD measurements could be improved by taking into account the effects of boundary layer height and relative humidity (Glantz et al., 2009).

For the active remote sensing, the first results from a one year campaign of lidar measurements of aerosol vertical profiles in Gual Pahari, India are presented in Paper V. Measurements were done with a seven-channel Raman lidar called Polly^{XT}. Polly^{XT} measured on 183 days for almost 2500 hours in total. From these measurements we calculated close to 500 one-hour average profiles. Our aim was to calculate an averaged profile every three hours. However, this requirement was limited by rain, low level clouds/fog and technical issues. The data was split into four seasons: spring (Mar-May), summer (Jun-Aug), autumn (Sep-Nov) and winter (Dec-Feb). The vertical profiles of backscatter, extinction, and lidar ratio and their variability during each season were calculated. The measurements revealed that the aerosol layer thickness followed mainly the seasonal pattern of temperature and, on average, the aerosol layer was at its highest in spring (5.5 km). In summer, the vertically averaged backscatter and extinction coefficients had the highest values (3.3 $Mm^{-1}sr^{-1}$ and 142 Mm^{-1} at 532 nm, respectively) when averaged over the 1-3 km height. Aerosol concentrations were slightly higher in summer compared with other seasons, and particles were larger in size. The autumn showed the highest lidar ratio (60 sr at 532 nm) and high extinction-related AE, indicating the presence of smaller probably absorbing particles. The winter had the lowest backscatter and extinction coefficients, but extinction-related AE was

the highest (1.03), suggesting still a large amount of small particles. These results are in good agreement with previous studies from the same region.

5 CONCLUSIONS

Optical remote sensing methods offer a wide range of instruments which can be used in the measurement of atmospheric aerosols. The aim of this research was to evaluate and use a number of these instruments over land.

The actual objectives of this research were listed in Chapter 1. The first objective was to evaluate the quality of the aerosol properties derived from the studied remote sensing instruments and to study the restrictions of these measurements over land. As presented in Paper I, accurate aerosol extinction retrievals can be done only if the assumed aerosol model is suitable for the studied area. However, satellite retrieval algorithms are global, thus aerosol models can only be indicative. This can lead to large discrepancies in the AOD at specific areas. Even though satellite retrievals suffer from these uncertainties, the MODIS AOD is a reliable parameter as shown in Paper II. Moreover, Paper IV indicated that MODIS AOD could be used as an estimate for $PM_{2.5}$ in Finland. For the active instruments, Paper III showed that aerosol model typing in the CALIOP retrieval works reliably only for dust aerosols. This indicates that all the more sophisticated aerosol parameters, e.g. AOD, have large uncertainties. However, based on recent studies (e.g. Kim et al. (2008b)), the location of the aerosol layers is reliably retrieved. In addition to aerosol model assumptions, the surface assumptions are vital. Paper II showed that the flawed surface reflectance assumptions in the MODIS retrieval are the reason for the failing of the AE retrieval.

The second objective was to find ways to improve the aerosol measurements done with the studied remote sensing instruments. Before realistic aerosol models can be applied into the aerosol retrieval algorithms, they have to be measured. Despite our extensive measurement campaign in Lakiala (Paper I) we were not able to calculate the observed aerosol extinction based on the measured aerosol size distributions because too many parameters were still unknown. As Paper I showed, for accurate aerosol extinction modeling, the assumed aerosol size distributions, refractive indices and growth factors have to coincide with the reality. In order to develop aerosol models more suitable for Finland, more measurements are needed. Overall, the correct aerosol model selection in satellite algorithms improves the aerosol retrievals, as discussed in Paper II. In the MODIS retrieval the improvement of the surface reflectance assumptions improved AE retrievals, as shown in Paper II. However, this improvement did not necessarily improve AOD retrieval. Actually, the AOD retrieval even deteriorated at some studied sites when AE retrieval was improved.

As for the active instruments, Paper III showed that CALIOP aerosol selection scheme had difficulties with almost all aerosol types, except dust. We studied if the scheme could be improved by introducing additional parameters into it. For this, we considered color ratio, which provides some information on the size of the aerosols. However, the variability of the parameter was large, thus the utilization of color ratio did not add more univocal information. Unfortunately, CALIOP does not have Raman

channels which would give information on the absorption properties of the aerosols. In the future missions, this should be taken into account.

The third objective was to use remote sensing measurements in the study of regional aerosol properties. This was achieved by studying the usability of AOD as an estimate for $PM_{2.5}$ in Helsinki, Finland (Paper IV). We found conversion factors which could be used to estimate $PM_{2.5}$ level from AOD measurements in this region. Our conversion factors were in line with results from other studies. In addition, we analyzed vertical aerosol profiles from lidar measurement done in Gual Pahari, India (Paper V). The seasonally averaged aerosol profiles showed how the height and properties of aerosols changed during the year. This information can be used to evaluate climate model parametrizations in this region.

With relation to the objectives of this thesis, there are several areas that require further work and research. Firstly, the identification of aerosol types is important because different aerosol types have different effects on health, visibility and climate change. When aerosol types are known, their sources can be identified more precisely and actions can be better targeted to reduce harmful aerosol emissions. Consequently, methods for aerosol type classification should be studied further. For example, the combination of remote sensing measurements and aerosol dispersion models could give valuable information on different aerosols.

Secondly, the possibility to improve the MODIS AE retrieval with better surface reflectance assumptions should be studied further. The surface assumptions could be evaluated in more detail with MODIS surface albedo data. These results could then also be utilized with other satellite instruments. Furthermore, the suitability of the assumed aerosol models for different locations should be studied globally.

Thirdly, the relationship of $PM_{2.5}$ and AOD in Northern Europe should be studied further with a longer time series. In addition, ground based AOD instruments could be used side by side with the satellite measurements. Moreover, vertical profiles of the aerosols should be added to the analysis. The profiles can be from lidar measurements or from global chemical transport models (van Donkelaar et al., 2010).

Fourthly, the development of aerosol models better suited for Finland could be based on the measurements presented in Paper I. However, more measurements of aerosol optical properties and vertical profiles should be done in parallel with size distribution measurements. Derived aerosol models could be utilized in the forecasting of "aerosol weather".

Fifthly, Polly^{XT} has been measuring constantly, thus more data is available for analysis. In addition, the retrieval of aerosol microphysics can be done from the best measurements. It will add invaluable information to the analysis. Furthermore, a method for aerosol type classification in a similar manner as in CALIOP but with information on extinction, could be developed for the instrument.

Lastly, one way to gather more information from the remote sensing instruments is to combine data from simultaneous measurement done with different instruments. Encouraging examples of these synergistic methods have been published by Satheesh

et al. (2009), Lee et al. (2007), Jeong and Hsu (2008), Torres et al. (2010) and Chatterjee et al. (2010). In addition, proxies, e.g. trace gases, can be used to locate specific types of aerosols. For example, SO_2 measurements can be used to locate volcanic ash plumes (Krueger et al. (2009); Heue et al. (2010); Karangulian et al. (2010)). Chen, B. et al. (2010) showed that CALIOP dust detection method misclassifies 43 % of the dust layers as clouds over Taklamakan desert. With the synergistic use of a passive Infrared Image Radiometer (IIR) they could reduce the misclassification rate to as low as $\sim$7 %. As these examples show, limitations of a single instrument can be compensated for by combining data from several instruments.

Two satellites carrying advanced instruments for aerosol measurements will be launched in the near future. In February 2011 NASA (National Aeronautics and Space Administration) will launch Glory satellite which will carry several instruments including Aerosol Polarimetry Sensor (APS). APS will measure the amount, size, refractive index, and shape of aerosols. It will be the first spaceborne instrument which is able to identify different aerosol types and discriminate between anthropogenic and natural aerosols (NASA (2010); Mischenko (2004)). ESA (European Space Agency), on the other hand, is planning to launch EarthCARE (Earth Clouds, Aerosols, and Radiation Explorer) satellite in 2013. This satellite will carry a backscatter lidar (ATLID) and a Multi spectral imager (MSI) among other instruments. The lidar and the imager will provide information on the occurrence of aerosols layers, their extinction coefficient profiles and boundary layer height. In addition, the instruments will be able to distinguish between absorbing and non-absorbing aerosols (ESA (2010); Hélière et al. (2007)). These missions will take spaceborne remote sensing a step further by providing more detailed information on the absorption, vertical location and size of aerosols.

References

Althausen, D., R. Engelmann, H. Baars, B. Heese, A. Ansmann, D. M uller, and M. Komppula (2009). Portable Raman Lidar Polly^{XT} for Automated Profiling of Aerosol Backscatter, Extinction, and Depolarization. *J. Atmos. Oceanic Technol., 26*, 2366-2378.

Anderson, T. L., R. J. Charlson, D. M. Winker, J. A. Ogren, and K. Holmén (2003). Mesoscale Variations of Tropospheric Aerosols. *J. Atmos. Sci., 60*, 119–136.

Anderson, T. L., R. J. Charlson, N. Bellouin, O. Boucher, M. Chin, S. A. Christopher, J. Haywood, Y. J. Kaufman, S. Kinne, J. A. Ogren, L. A. Remer, T. Takemura, D. Tanré, O. Torres, C. R. Trepte, B. A. Wielicki, D. A. Winker, and H. Yu (2005). An A-Train Strategy for Quantifying Direct Climate Forcing by Anthropogenic Aerosols. *Bull. Amer. Meteor. Soc., 18*, 1795-1809.

Ansmann, A., M. Tesche, S. Groß, V. Freudenthaler, P. Seifert, A. Hiebsch, J. Schmidt, U. Wandinger, I. Mattis, D. Müller, and M. Wiegner (2010). The 16 April 2010 major volcanic ash plume over central Europe: EARLINET lidar and AERONET photometer observations at Leipzig and Munich, Germany. *Geophys. Res. Lett., 37*, L13810, doi:10.1029/2010GL043809.

Bond, T. and R. Bergstrom (2006). Light Absorption by Carbonaceous Particles: An Investigative Review. *Aerosol Sci. Technol., 40*, 27–67.

Bréon, F.-M., D. Tanré, and S. Generoso (2002). Aerosol Effect on Cloud Droplet Size Monitored from Satellite. *Science, 295*, 834-838

Burton, S. P., R. A. Ferrare, C. A. Hostetler, J. W. Hair, C. Kittaka, M. A. Vaughan, M. D. Obland, R. R. Rogers, A. L. Cook, D. B. Harper, and L. A. Remer (2010). Using airborne high spectral resolution lidar data to evaluate combined active plus passive retrievals of aerosol extinction profiles. *J. Geophys. Res., 115*, D00H15, doi:10.1029/2009JD012130.

Carlund, T., T. Landelius, and W. Josefsson (2003). Comparison and uncertainty of aerosol optical depth estimates derived from spectral and broadband measurements. *J. Appl. Meteorol., 42*, 1598–1610.

Charlson, R. J., S. E. Schwartz, J. M. Hales, R.D. Cess, J. A. Coakley Jr., J. E. Hansen, and D. J. Hofmann (1992). Climate Forcing by Anthropogenic Aerosols. *Science, 255*, 423–430.

Chatterjee, A., A. M. Michalak, R. A. Kahn, S. R. Paradise, A. J. Braverman, and C. E. Miller (2010). A Geostatistical Data Fusion Technique for Merging Remote Sensing and Ground-based Observations of Aerosol Optical Thickness. *J. Geophys. Res.*, doi:10.1029/2009JD013765, in press.

Chen, B., J. Huang, P. Minnis, Y. Hu, Y. Yi, Z. Liu, D. Zhang, and X. Wang (2010). Detection of dust aerosol by combining CALIPSO active lidar and passive IIR measurements. *Atmos. Chem. Phys., 10*, 4241-4251, doi:10.5194/acp-10-4241-2010.

Chen, W.-T., A. Nenes, H. Liao, P. J. Adams, J.-L. F. Li, and J. H. Seinfeld (2010). Global climate response to anthropogenic aerosol indirect effects: Present day and year 2100. *J. Geophys. Res., 115*, D12207, doi:10.1029/2008JD011619

Christopher S. A., and P. Gupta (2010). Satellite Remote Sensing of Particulate Matter Air Quality: The Cloud-Cover Problem. *J. Air & Waste Manage. Assoc., 60*, 5, 596-602.

Chung, C. E., V. Ramanathan, G. Carmichael, S. Kulkarni, Y. Tang, B. Adhikary, L. R. Leung, and Y. Qian (2010). Anthropogenic aerosol radiative forcing in Asia derived from regional models with atmospheric and aerosol data assimilation. *Atmos. Chem. Phys., 10*, 6007-6024, doi:10.5194/acp-10-6007-2010.

de Leeuw, G., M. Sofiev, J. Vira, J. Tamminen, L. Sogacheva, A.-M. Sundström, P. Kolmonen, E. Rodriguez, W. von Hoyningen- Huene, A. Arola, T. Mielonen, J. Hakkarainen, V.-M. Kerminen, D. Rosenfeld, L. A. Remer, R. A. Kahn (2010). Using satellite data to obtain information on the Eyjafjallajökull ash plume. *EGU 2010*, Abstract 15738.

Delene, D. J., and J. A. Ogren (2002). Variability of Aerosol Optical Properties at Four North American Surface Monitoring Sites. *J. Atmos. Sci., 59*, 1135–1150.

Deuzé, J., F. M. Bréon, C. Devaux, P. Goloub, M. Herman, B. Lafrance, F. Maignan, A. Marchand, F. Nadal, G. Perry, and D. Tanré (2001). Remote sensing of aerosols over land surfaces from POLDER-ADEOS-1 polarized measurements. *J. Geophys. Res., 106*, D5, 4913-4926.

Di Nicolantonio, W., A. Cacciari, S. Scarpanti, G. Ballista, E. Morisi, and R. Guzzi (2006). SCIAMACHY TOA reflectance correction effects on aerosol optical depth retrieval. *Proc. of the First Atmospheric Science Conference, ESA SP-628*, 8–12 May 2006–ESA ESRIN.

Dickerson, R. R., S. Kondragunta, G. Stenchikov, K. L. Civerolo, B. G. Doddridge, and B. N. Holben (1997). The Impact of Aerosols on Solar Ultraviolet Radiation and Photochemical Smog. *Science, 278*, 827–830.

Diner, D. J., J. V. Martonchik, R. A. Kahn, B. Pinty, N. Gobron, D. L. Nelson, B. N. Holben (2005). Using angular and spectral shape similarity constraints to improve MISR aerosol and surface retrievals over land. *Remote Sens. Environ., 94*, 2, 155-171, ISSN 0034-4257, DOI: 10.1016/j.rse.2004.09.009.

Dubovik O., and M. King (2000). A flexible inversion algorithm for retrieval of aerosol optical properties from Sun and sky radiance measurements. *J. Geophys. Res., 105*, D16, doi:10.1029/2000JD900282.

Dubovik, O., M. Herman, A. Holdak, T. Lapyonok, D. Tanré, J.-L. Deuzé, F. Ducos, A. Sinyuk, and A. Lopatin (2010). Development of statistically optimized inversion algorithm for enhanced retrieval of aerosol properties from spectral multi-angle polarimetric satellite observations. *Atmos. Meas. Tech. Discuss.*, in preparation.

Eck, T., B. Holben, J. Reid, O. Dubovik, A. Smirnov, N. O'Neill, I. Slutsker, S. Kinne (1999). Wavelength dependence of the optical depth of biomass burning, urban, and desert dust aerosols. *J. Geophys. Res., 104*, 31,333–31,349.

European Space Agency. ESA's cloud and aerosol mission EarthCare. Available at: http://www.esa.int/esaLP/ASESMYNW9SC_LPearthcare_0.html. Cited 13th October 2010.

Fernald, F.G. (1984). Analysis of atmospheric lidar observations: Some comments. *Appl. Opt., 23*, 652–653, doi:10.1364/AO.23.000652.

Ferrare, R. A., D. D. Turner, L. Heilman Brasseur, W. F. Feltz, O. Dubovik, and T. P. Tooman (2001). Raman lidar measurements of the aerosol extinction-to-backscatter ratio over the Southern Great Plains. *J. Geophys. Res., 106*, 20,333–20,347.

Fuzzi, S., M. O. Andreae, B.J. Huebert, M. Kulmala, T. C. Bond, M. Boy, S. J. Doherty, A. Guenther, M. Kanakidou, K. Kawamura, V.-M. Kerminen, U. Lohmann, L. M. Russell, and U. Pöschl (2006). Critical assessment of the current state of scientific knowledge, terminology, and research needs concerning the role of organic aerosols in the atmosphere, climate, and global change. *Atmos. Chem. Phys., 6*, 2017-2038, doi:10.5194/acp-6-2017-2006.

Glantz, P., A. Kokhanovsky, W. von Hoyningen-Huene, and C. Johansson (2009). Estimating PM2.5 over southern Sweden using space-borne optical measurements. *Atmos. Environ., 43*, 5838–5846.

Grey W. M. F., P. R. J. North, and S. O. Los (2006). Computationally efficient method for retrieving aerosol optical depth from ATSR-2 and AATSR data. *Appl. Opt., 45*, 12, 2786-2795.

Hélière, A., A. Lefebvre, T. Wehr, J. L. Bézy, and Y. Durand (2007). The EarthCARE mission: Mission concept and lidar instrument pre-development. IEEE International Geoscience and Remote Sensing Symposium (IGARSS), Proceeding paper, 4975–4978.

Heue, K.-P., C. A. M. Brenninkmeijer, T. Wagner, K. Mies, B. Dix, U. Frieß, B. G. Martinsson, F. Slemr, and P. F. J. van Velthoven (2010). Observations of the 2008

Kasatochi volcanic SO2 plume by CARIBIC aircraft DOAS and the GOME-2 satellite. *Atmos. Chem. Phys., 10*, 4699-4713, doi:10.5194/acp-10-4699-2010.

Hinds, W. (1998). *Aerosol Technology. Properties, behavior, and measurement of airborne particles*, 2nd ed., John Wiley & Sons, Inc., New York, USA.

Holben, B. N., T. F. Eck, I. Slutsker, D. Tanré, J. P. Buis, A. Setzer, E. Vermote, J. A. Reagan, Y. J. Kaufman, T. Nakajima, F. Lavenu, I. Jankowiak and A. Smirnov (1998). AERONET–A federated instrument network and data archive for aerosol characterization. *Remote Sens. Environ., 66*, 1–16.

Hsu, N. C., S. C. Tsay, M. D. King, and J. R. Herman (2006). Deep blue retrievals of Asian aerosol properties during ACE-Asia. *IEEE T. Geosci. Remote Sens., 44*, 3180–3195.

Hågård, A., and R. Persson (1992). Infrared Transmission Measurement in the Atmosphere. *SPIE* Vol. 1762 Infrared Technology XVIII.

IPCC (2007). Summary for policy makers, in *Climate Change 2007: The physical Science Basis. Contribution of Working Group I to the Fourth Assessment Report of the Intergovernmental Panel on Climate Change*, edited by S. Solomon, D. Qin, M. Manning, Z. Chen, M. Marquis, K. Averyt, M. Tignor, and H. Miller, Cambridge University Press, Cambridge, United Kingdom and New York, USA.

Jeong, M., and N. C. Hsu (2008). Retrievals of aerosol single-scattering albedo and effective aerosol layer height for biomass-burning smoke: Synergy derived from "A-Train" sensors. *Geophys. Res. Lett., 35*, L24801, doi:10.1029/2008GL036279.

Kahn, R. A., P. Banerjee, and D. McDonald (2001). Sensitivity of multiangle imaging to natural mixtures of aerosols over ocean. *J. Geophys. Res., 106*, 18219–18238.

Kahn, R. A., Y. Chen, D. L. Nelson, F.-Y. Leung, Q. Li, D. Diner, and J. A. Logan (2008). Wildfire smoke injection heights: Two perspectives from space. *Geophys. Res. Lett., 35*, 04.

Kan, H. D., and B. H. Chen (2002). Analysis of exposure-response relationships of air particulate matter and adverse health outcomes in China. *J. of Environ. Health, 19*, 422–424.

Karagulian, F., L. Clarisse, C. Clerbaux, A. J. Prata, D. Hurtmans, and P. F. Coheur (2010). Detection of volcanic SO2, ash, and H2SO4 using the Infrared Atmospheric Sounding Interferometer (IASI). *J. Geophys. Res., 115*, D00L02, doi:10.1029/2009JD012786.

Kaufman, Y., D. Tanré, L. A. Remer, E. Vermote, A. Chu, and B. N. Holben (1997). Operational remote sensing of tropospheric aerosol over land from EOS moderate resolution imaging spectroradiometer. *J. Geophys. Res., 102*, D14, 17051-17067.

Kaurila, T., A. Hågård, and R. Persson (2006). Aerosol Extinction Models based on measurements at two sites in Sweden. *Appl. Opt., 45*, 26, 6750-6761.

Keller, J., S. Bojinski, and A. S. H. Prevot (2007). Simultaneous retrieval of aerosol and surface optical properties using data of the Multiangle Imaging SpectroRadiometer (MISR). *Remote Sens. Environ., 107*, 120–137.

Kim, S.-W., S.-C. Yoon, E. G. Dutton, J. Kim, C. Wehrli and B. N. Holben (2008a). Global Surface-Based Sun Photometer Network for Long-Term Observations of Column Aerosol Optical Properties: Intercomparison of Aerosol Optical Depth. *Aerosol Sci. Technol., 42*, 1, 1–9.

Kim, S.-W., S. Berthier, J.-C. Raut, P. Chazette, F. Dulac, and S.-C. Yoon (2008b). Validation of aerosol and cloud layer structures from the space-borne lidar CALIOP using a ground-based lidar in Seoul, Korea. *Atmos. Chem. Phys., 8*, 3705–3720.

Klett, J. D. (1981). Stable analytical inversion solution for processing lidar returns. *Appl. Opt., 20*, 211–220, doi:10.1364/AO.20.000211.

Kokhanovsky A. A., F.-M. Bréon, A. Cacciari, E. Carboni, D. Diner, W. Di Nicolantonio, R. G. Grainger, W. M. F. Grey, R. Holler, K.-H. Lee, Z. Li, P. R. J. North, A. M. Sayer, G. E. Thomas, W. von Hoyningen-Huene (2007). Aerosol remote sensing over land: A comparison of satellite retrievals using different algorithms and instruments. *Atmos. Res., 85*, 3–4, 372–394, DOI: 10.1016/j.atmosres.2007.02.008.

Kokhanovsky, A. A., J. L. Deuzé, D. J. Diner, O. Dubovik, F. Ducos, C. Emde, M. J. Garay, R. G. Grainger, A. Heckel, M. Herman, I. L. Katsev, J. Keller, R. Levy, P. R. J. North, A. S. Prikhach, V. V. Rozanov, A. M. Sayer, Y. Ota, D. Tanré, G. E. Thomas, and E. P. Zege (2010). The inter-comparison of major satellite aerosol retrieval algorithms using simulated intensity and polarization characteristics of reflected light. *Atmos. Meas. Tech., 3*, 909-932, doi:10.5194/amt-3-909-2010.

Krueger, A. J., N. A. Krotkov, K. Yang, S. Carn, G. Vicente, and W. Schroeder (2009). Applications of Satellite-Based Sulfur Dioxide Monitoring. *IEEE J. Selected Topics in Applied Earth Observations and Remote Sensing, 2*, 4, 293-298.

Lee, K. H., Y. J. Kim, W. von Hoyningen-Huene, J. P. Burrow (2006). Influence of land surface effects on MODIS aerosol retrieval using the BAER method over Korea. *Int. J. Remote Sens., 27*, 2813–2830.

Lee, J., J. Kim, H. C. Lee, and T. Takemura (2007). Classification of Aerosol Type from MODIS and OMI over East Asia. *J. Korean Meteor. Soc., 43*, 343–357

Lee, K. H, Z. Li, Y. J. Kim, and A. A. Kokhanovsky (2009). Atmospheric aerosol monitoring form satellite observations: a history of three decades, in *Atmospheric*

and Biological Environmental Monitoring, edited by Kim, Y.J, Platt, U., Gu, M.B, and Iwawashi, H., Springer, Berlin, 13–38.

Levy, R. C., L.A. Remer, S. Mattoo, E. F. Vermote and Y. J. Kaufman (2007). Second-generation operational algorithm: Retrieval of aerosol properties over land from inversion of Moderate Resolution Imaging Spectroradiometer spectral reflectance. *J. Geophys. Res., 112*, D13211.

Levy, R. C. (2009). The dark-land MODIS collection 5 aerosol retrieval: algorithm development and product evaluation, in: *Satellite Aerosol Remote Sensing over Land*, edited by Kokhanovsky, A.A. and de Leeuw, G., Springer-Praxis, Berlin, 19–68.

Levy, R. C., L. A. Remer, R. G. Kleidman, S. Mattoo, C. Ichoku, R. Kahn and T. F. Eck (2010). Global evaluation of the Collection 5 MODIS aerosol products over land and ocean. *Atmos. Chem. Phys. Disc., 10*, 14815–14873.

Li, J. J., L. Y. Shao, and S. S. Yang (2006). Adverse effect mechanisms of inhalable particulate matters. *J. Environ.Health, 3*, 185–188.

Liou, K. N. (2002). *An Introduction to Atmospheric Radiation*, 2nd ed., Academic Press, San Diego, USA.

Lubin, D., and A. M. Vogelmann (2010). Observational quantification of a total aerosol indirect effect in the Arctic. *Tellus B, 62*, 3, 181-189.

Mishchenko, M. I., B. Cairns, J. E. Hansen, L. D. Travis, R.d Burg, Y. J. Kaufman, J. V. Martins, E. P. Shettle (2004). Monitoring of aerosol forcing of climate from space: analysis of measurement requirements. *J. Quant. Spectrosc. Radiat. Transfer, 88*, 149-161.

National Aeronautics and Space Administration. Glory - Observing the Earth's Aerosols and Solar Irradiance. Available at: http://glory.gsfc.nasa.gov/misison_details.html. Cited 13th October 2010.

Omar, A. H., D. M. Winker, M. A. Vaughan, Y. Hu, C. R. Trepte, R. A. Ferrare, K.-P. Lee, C. A. Hostetler, C. Kittaka, R. R. Rogers, R. E. Kuehn, and Z. Liu (2009). The CALIPSO automated aerosol classification and lidar ratio selection algorithm. *J. Atmos. Oceanic Technol., 26*, 1994–2014, doi:10.1175/2009JTECHA1231.1.

Penner, J. E., R. E. Dickinson, and C. A. O'Neill (1992). Effects of Aerosol from Biomass Burning on the Global Radiation Budget. *Science, 256*, 1432–1434.

Petty, G. W. (2006). *First course in atmospheric radiation*, 2nd edition, Sundog Publishing, Madison, Wisconsin, ISBN 0-9729033-1-3.

Pope III, C. A. (2000). Review: epidemiological basis for particulate air pollution health standards. *Aerosol Sci. Technol., 32*, 4–14.

Pope III, C. A., and D. W. Dockery (2006). Health Effects of Fine Particulate Air Pollution: Lines that Connect. *J. Air & Waste Manag. Assoc., 56*, 709–742.

Quaas, J., Y. Ming, S. Menon, T. Takemura, M. Wang, J. E. Penner, A. Gettelman, U. Lohmann, N. Bellouin, O. Boucher, A. M. Sayer, G. E. Thomas, A. McComiskey, G. Feingold, C. Hoose, J. E. Kristjánsson, X. Liu, Y. Balkanski, L. J. Donner, P. A. Ginoux, P. Stier, B. Grandey, J. Feichter, I. Sednev, S. E. Bauer, D. Koch, R. G. Grainger, A. Kirkevåg, T. Iversen, Ø. Seland, R. Easter, S. J. Ghan, P. J. Rasch, H. Morrison, J.-F. Lamarque, M.J. Iacono, S. Kinne, and M. Schulz (2009). Aerosol indirect effects – general circulation model intercomparison and evaluation with satellite data. *Atmos. Chem. Phys., 9*, 8697–8717, doi:10.5194/acp-9-8697-2009.

Quaas, J., B. Stevens, P. Stier, and U. Lohmann (2010). Interpreting the cloud cover – aerosol optical depth relationship found in satellite data using a general circulation model. *Atmos. Chem. Phys., 10*, 6129–6135, doi:10.5194/acp-10-6129-2010.

Remer, L. A., Y. J. Kaufman, D. Tanré, S. Mattoo, D. A. Chu, J. V. Martins, R.-R. Lee, C. Ichoku, R. C. Levy, R. G. Kleidman, T. F. Eck, E. Vermote, and B. N. Holben (2005). The MODIS aerosol algorithm, products, and validation. *J. Atmos. Sci., 62*, 4, 947–973.

Rozanov, V. V. and A.V. Rozanov (2010). Differential optical absorption spectroscopy (DOAS) and air mass factor concept for a multiply scattering vertically inhomogeneous medium: theoretical consideration. *Atmos. Meas. Tech., 3*, 751–780, doi:10.5194/amt-3-751-2010.

Salomonson, V. V., W. L. Barnes, P. W. Maymon, H. E. Montgomery, and H. Ostrow (1989). MODIS, advanced facility instrument for studies of the Earth as a system. *IEEE T. Geosci. Remote Sens., 27*, 145–153.

Sano, I., M. Mukai, N. Iguchi, and S. Mukai (2010). Suspended particulate matter sampling at an urban AERONET site in Japan, part 2: relationship between column aerosol optical thickness and PM2.5 concentration. *J. Appl. Remote Sens., 4*, 043504.

Santer, R., V. Carrere, P. Dubuisson, and J. C. Rogers (1999). Atmospheric corrections over land for MERIS. Int. *J. Remote Sens., 20*, 1819–1840.

Santer R., et al. (2000). Atmospheric product over land for MERIS level 2. *MERIS Algorithm Theoretical Basis Document, ATBD 2.15*, ESA.

Sasano, Y., E. V. Browell, and S. Ismail (1985). Error caused by using a constant extinction/backscattering ratio in the lidar solution. *Appl. Opt., 24*, 3929–3932, doi:10.1364/AO.24.003929.

Sassen, K. (2005). Polarization Lidar, In *Lidar: Range-Resolved Optical Remote Sensing of the Atmosphere*, edited by C. Weitkamp. Springer, ISBN 0-387-40075-3.

Satheesh, S. K., O. Torres, L. A. Remer, S. S. Babu, V. Vinoj, T. F. Eck, R. G. Kleidman, and B. N. Holben (2009). Improved assessment of aerosol absorption using OMI-MODIS joint retrieval. *J. Geophys. Res., 114*, D05209, doi:10.1029/2008JD011024

Schaepman-Strub, G., M. E. Schaepman, T. H. Painter, S. Dangel, and J.V. Martonchik (2006). Reflectance quantities in optical remote sensing - definitions and case studies. *Remote Sens. Environ., 103*, 27–42.

Schuster, G. L., O. Dubovik, and B. N. Holben (2006). Angstrom exponent and bimodal aerosol size distributions. *J. Geophys. Res., 111*, D07207.

Schwartz, S. E., R. J. Charlson, R. A. Kahn, J. A. Ogren, H. Rodhe (2010). Why Hasn't Earth Warmed as Much as Expected?. *J. Climate, 23*, 2453–2464.

Seinfeld, J., and S. Pandis (2006). *Atmospheric chemistry and physics. From air pollution to climate change*, 2nd ed., Wiley & Sons, Inc., New York, USA.

Stone, R. S., A. Herber, V. Vitale, M. Mazzola, A. Lupi, R. C. Schnell, E. G. Dutton, P. S. K. Liu, S.-M. Li, K. Dethloff, A. Lampert, C. Ritter, M. Stock, R. Neuber (2010). A three-dimensional characterization of Arctic aerosols from airborne Sun photometer observations: PAM-ARCMIP. *J. Geophys. Res., 115*, D13203, doi:10.1029/2009JD013605.

Thomas, G. E., C. A. Poulsen, A. M. Sayer, S. H. Marsh, S. M. Dean, E. Carboni, R. Siddans, R. G. Grainger, and B. N. Lawrence (2009). The GRAPE aerosol retrieval algorithm. *Atmos. Meas. Tech., 2*, 679–701, doi:10.5194/amt-2-679-2009

Torres, O., A. Tanskanen, B. Veihelmann, C. Ahn, R. Braak, P. K. Bhartia, P. Veefkind, and P. Levelt (2007). Aerosols and surface UV products from Ozone Monitoring Instrument observations: An overview. *J. Geophys. Res., 112*, D24S47, doi:10.1029/2007JD008809.

Torres, O., Z. Chen, H. Jethva, C. Ahn, S. R. Freitas, and P. K. Bhartia (2010). OMI and MODIS observations of the anomalous 2008–2009 Southern Hemisphere biomass burning seasons. *Atmos. Chem. Phys., 10*, 3505-3513, doi:10.5194/acp-10-3505-2010.

Wagner, T., T. Deutschmann, and U. Platt (2009). Determination of aerosol properties from MAX-DOAS observations of the Ring effect. *Atmos. Meas. Tech., 2*, 495–512, doi:10.5194/amt-2-495-2009.

Wallace, L. (2000). Correlations of personal exposure to particles with outdoor air measurement: A review of recent studies. *Aerosol Sci. Technol., 32*, 15–25.

van der Meulen, P. (1992). Visibility measuring instruments: Difference between scatterometers and transmissometers. Instruments and Observing Methods. *Report No. 49*, (WMO/TD -No. .462), pp. 331.

van Donkelaar A, R. V. Martin, M. Brauer, R. Kahn, R. Levy, C. Verduzco, and P.J. Villeneuve (2010). Global Estimates of Ambient Fine Particulate Matter Concentrations from Satellite-Based Aerosol Optical Depth: Development and Application. *Environ Health Perspect, 118*, 6, doi:10.1289/ehp.0901623.

Wandinger, U. (2005a). Introduction to Lidar, In *Lidar: Range-Resolved Optical Remote Sensing of the Atmosphere*, edited by C. Weitkamp. Springer, ISBN 0-387-40075-3.

Wandinger, U. (2005b). Raman Lidar, In *Lidar: Range-Resolved Optical Remote Sensing of the Atmosphere*, edited by C. Weitkamp. Springer, ISBN 0-387-40075-3.

Vaughan, M., S. Young, D. Winker, K. Powell, A. Omar, Z. Liu, Y. Hu and C. Hostetler (2004). Fully automated analysis of space-based lidar data: an overview of the CALIPSO retrieval algorithms and data products. *Proc. SPIE, 5575*, pp. 16–30.

Weber, S. A., J. A. Engel-Cox, R. M. Hoff, A. I. Prados, and H. Zhang (2010). An Improved Method for Estimating Surface Fine Particle Concentrations Using Seasonally Adjusted Satellite Aerosol Optical Depth. *J. Air & Waste Manag. Assoc., 60*, 5, 574–585

Wehrli, C. (2000). Calibrations of Filter Radiometers for Determination of Atmospheric Optical Depth. *Metrologia, 37*, 419–422.

Welton, E. J., J. R. Campbell, J. D. Spinhirne, and V. S. Scott (2001). Global monitoring of clouds and aerosols using a network of micro-pulse lidar systems, in *Lidar Remote Sensing for Industry and Environmental Monitoring*, U. N. Singh, T. Itabe, N. Sugimoto, (eds.), Proc. SPIE, 4153, 151–158.

Whyte, C., R. J. Leigh, D. Lobb, T. Williams, J. J. Remedios, M. Cutter, and P.S. Monks (2009). Assessment of the performance of a compact concentric spectrometer system for Atmospheric Differential Optical Absorption Spectroscopy. *Atmos. Meas. Tech., 2*, 789-800, doi:10.5194/amt-2-789-2009.

Wiegner, M., J. Bösenberg, C. Böckmann, R. Eixmann, V. Freudenthaler, I. Mattis, T. Trickl (1999). Lidar network to establish an aerosol climatology. *J. Aerosol Sci., 30*, Suppl. 1, S429–S430.

Winker, D. M., J. Pelon and M. P. McCormick (2003). The CALIPSO mission: spaceborne lidar for observation of aerosols and clouds. *Proc. SPIE, 4893*, pp. 1–11.

Winker, D. M., W. H. Hunt, and M. J. McGill (2007). Initial performance assessment of CALIOP. *Geophys. Res. Lett., 34*, L19803.

Winker, D. M., M. A. Vaughan, A. Omar, Y. Hu, K. A. Powell, Z. Liu, W. H. Hunt, and S. A. Young (2009). Overview of the CALIPSO mission and

CALIOP data processing algorithms. *J. Atmos. Oceanic Technol., 26*, 2310–2323, doi:10.1175/2009JTECHA1281.1.

Volz, F. E. (1959). Photometer mit Selen-photoelement zurspektralen Messung der Sonnenstrahlung und zer Bestimmung der Wallenlangenabhangigkeit der Dunsttrubung. Arch. *Meteorol. Geophys. Bioklim., B10*, 100–131.

von Hoyningen-Huene, W., M. Freitag, and J. B. Burrows (2003). Retrieval of aerosol optical thickness over land surfaces from top-of-atmosphere radiance. *J. Geophys. Res., 108*, D9, 4260, doi:10.1029/2001JD002018.

Young, S. A., and M. A. Vaughan (2009). The retrieval of profiles of particulate extinction from Cloud-Aerosol Lidar Infrared Pathfinder Satellite Observations (CALIPSO) data: Algorithm description. *J. Atmos. Oceanic Technol., 26*, 1105–1119, doi:10.1175/2008JTECHA1221.1.

Ångström, A. (1929). On the atmospheric transmission of Sun radiation and on dust in the air. *Geogr. Ann., 11*, 156–166.

Finnish Meteorological Institute Contributions

1. Joffre, Sylvain M., 1988. Parameterization and assessment of processes affecting the long-range transport of airborne pollutants over the sea. 49 p.

2. Solantie, Reijo, 1990. The climate of Finland in relation to its hydrology, ecology and culture. 130 p.

3. Joffre, Sylvain M. and Lindfors, Virpi, 1990. Observations of airborne pollutants over the Baltic Sea and assessment of their transport, chemistry and deposition. 41 p.

4. Lindfors, Virpi, Joffre, Sylvain M. and Damski, Juhani, 1991. Determination of the wet and dry deposition of sulphur and nitrogen compounds over the Baltic Sea using actual meteorological data. 111 p.

5. Pulkkinen, Tuija, 1992. Magnetic field modelling during dynamic magnetospheric processes. 150 p.

6. Lönnberg, Peter, 1992. Optimization of statistical interpolation. 157 p.

7. Viljanen, Ari, 1992. Geomagnetic induction in a one- or two-dimensional earth due to horizontal ionospheric currents. 136 p.

8. Taalas, Petteri, 1992. On the behaviour of tropospheric and stratospheric ozone in Northern Europe and in Antarctica 1987-90. 88 p.

9. Hongisto, Marke, 1992. A simulation model for the transport, transformation and deposition of oxidized nitrogen compounds in Finland — 1985 and 1988 simulation results. 114 p.

10. Taalas, Petteri, 1993. Factors affecting the behaviour of tropospheric and stratospheric ozone in the European Arctic and Antarctica. 138 s.

11. Mälkki, Anssi, 1993. Studies on linear and non-linear ion waves in the auroral acceleration region. 109 p.

12. Heino, Raino, 1994. Climate in Finland during the period of meteorological observations. 209 p.

13. Janhunen, Pekka, 1994. Numerical simulations of E-region irregularities and ionosphere-magnetosphere coupling. 122 p.

14. Hillamo, Risto E., 1994. Development of inertial impactor size spectroscopy for atmospheric aerosols. 148 p.

15. Pakkanen, Tuomo A., 1995. Size distribution measurements and chemical analysis of aerosol components. 157 p.

16. Kerminen, Veli-Matti, 1995. On the sulfuric acid-water particles via homogeneous nucleation in the lower troposphere. 101 p.

17. Kallio, Esa, 1996. Mars-solar wind interaction: Ion observations and their interpretation. 111 p.

18. Summanen, Tuula, 1996. Interplanetary Lyman alpha measurements as a tool to study solar wind properties. 114 p.

19. Rummukainen, Markku, 1996. Modeling stratospheric chemistry in a global three-dimensional chemical transport model, SCTM-1. Model development. 206 p.

20. Kauristie, Kirsti, 1997. Arc and oval scale studies of auroral precipitation and electrojets during magnetospheric substorms. 134 p.

21. Hongisto, Marke, 1998. Hilatar, A regional scale grid model for the transport of sulphur and nitrogen compounds. 152 p.

22. Lange, Antti A.I., 1999. Statistical calibration of observing systems. 134 p.

23. Pulkkinen, Pentti, 1998. Solar differential rotation and its generators: computational and statistical studies. 108 p.

24. Toivanen, Petri, 1998. Large-scale electromagnetic fields and particle drifts in time-dependent Earth's magnetosphere. 145 p.

25. Venäläinen, Ari, 1998. Aspects of the surface energy balance in the boreal zone. 111 p.

26. Virkkula, Aki, 1999. Field and laboratory studies on the physical and chemical properties of natural and anthropogenic tropospheric aerosol. 178 p.

27. Siili, Tero, 1999. Two-dimensional modelling of thermal terrain-induced mesoscale circulations in Mars' atmosphere. 160 p.

28. Paatero, Jussi, 2000. Deposition of Chernobyl-derived transuranium nuclides and short-lived radon-222 progeny in Finland. 128 p.

29. Jalkanen, Liisa, 2000. Atmospheric inorganic trace contaminants in Finland, especially in the Gulf of Finland area. 106 p.

30. Mäkinen, J. Teemu, T. 2001. SWAN Lyman alpha imager cometary hydrogen coma observations. 134 p.

31. Rinne, Janne, 2001. Application and development of surface layer flux techniques for measurements of volatile organic compound emissions from vegetation. 136 p.

32. Syrjäsuo, Mikko T., 2001. Auroral monitoring system: from all-sky camera system to automated image analysis. 155 p.

33. Karppinen, Ari, 2001. Meteorological pre-processing and atmospheric dispersion modelling of urban air quality and applications in the Helsinki metropolitan area. 94 p.

34. Hakola, Hannele, 2001. Biogenic volatile organic compound (VOC) emissions from boreal deciduous trees and their atmospheric chemistry. 125 p.

35. Merenti-Välimäki, Hanna-Leena, 2002. Study of automated present weather codes.153 p.

36. Tanskanen, Eija I., 2002. Terrestrial substorms as a part of global energy flow. 138 p.

37. Nousiainen, Timo, 2002. Light scattering by nonspherical atmospheric particles. 180 p.

38. Härkönen, Jari, 2002. Regulatory dispersion modelling of traffic-originated pollution. 103 p.

39. Oikarinen, Liisa, 2002. Modeling and data inversion of atmospheric limb scattering measurements. 111 p.

40. Hongisto, Marke, 2003. Modelling of the transport of nitrogen and sulphur contaminants to the Baltic Sea Region. 188 p.

41. Palmroth, Minna, 2003. Solar wind – magnetosphere interaction as determined by observations and a global MHD simulation. 147 p.

42. Pulkkinen, Antti, 2003. Geomagnetic induction during highly disturbed space weather conditions: Studies of ground effects 164 p.

43. Tuomenvirta, Heikki, 2004. Reliable estimation of climatic variations in Finland. 158 p.

44. Ruoho-Airola, Tuija, 2004. Temporal and regional patterns of atmospheric components affecting acidification in Finland. 115 p.

45. Partamies, Noora, 2004. Meso-scale auroral physics from groundbased observations. 122 p.

46. Teinilä, Kimmo, 2004. Size resolved chemistry of particulate ionic compounds at high latitudes. 138 p.

47. Tamminen, Johanna, 2004. Adaptive Markov chain Monte Carlo algorithms with geophysical applications. 156 p.

48. Huttunen, Emilia, 2005. Interplanetary shocks, magnetic clouds, and magnetospheric storms. 142 p.

49. Sofieva, Viktoria, 2005. Inverse problems in stellar occultation. 110 p.

50. Harri, Ari-Matti, 2005. In situ observations of the atmospheres of terrestrial planetary bodies. 246 p.

51. Aurela, Mika, 2005. Carbon dioxide exchange in subarctic ecosystems measured by a micrometeorological technique. 132 p.

52. Damski, Juhani, 2005. A Chemistry-transport model simulation of the stratospheric ozone for 1980 to 2019. 147 p.

53. Tisler, Priit, 2006. Aspects of weather simulation by numerical process. 110 p.

54. Arola, Antti, 2006. On the factors affecting short- and long-term UV variability. 82 p.

55. Verronen, Pekka T., 2006. Ionosphere-atmosphere interaction during solar proton events. 146 p.

56. Hellén, Heidi, 2006. Sources and concentrations of volatile organic compounds in urban air. 134 p.

57. Pohjola, Mia, 2006. Evaluation and modelling of the spatial and temporal variability of particulate matter in urban areas. 143 p.

58. Sillanpää, Markus, 2006. Chemical and source characterisation of size-segregated urban air particulate matter. 184 p.

59. Niemelä, Sami, 2006. On the behaviour of some physical parameterization methods in high resolution numerical weather prediction models. 136 p.

60. Karpechko, Alexey, 2007. Dynamical processes in the stratosphere and upper troposphere and their influence on the distribution of trace gases in the polar atmosphere. 116 p.

61. Eresmaa, Reima, 2007. Exploiting ground-based measurements of Global Positioning System for numerical weather prediction. 95 p.

62. Seppälä, Annika, 2007. Observations of production and transport of NOx formed by energetic particle precipitation in the polar night atmosphere. 100 p.

63. Rontu, Laura, 2007. Studies on orographic effects in a numerical weather prediction model. 151 p.

64. Vajda, Andrea, 2007. Spatial variations of climate and the impact of disturbances on local climate and forest recovery in northern Finland. 139 p.

65. Laitinen, Tiera, 2007. Rekonnektio Maan magnetosfäärissä – Reconnection in Earth's magnetosphere. 226 s.

66. Vanhamäki, Heikki, 2007. Theoretical modeling of ionospheric electrodynamics including induction effects. 170 p.

67. Lindfors. Anders, 2007. Reconstruction of past UV radiation. 123 p.

68. Sillanpää, Ilkka, 2008. Hybrid modelling of Titan's interaction with the magnetosphere of Saturn. 200 p.

69. Laine, Marko, 2008. Adaptive MCMC methods with applications in environmental and geophysical models. 146 p.

70. Tanskanen, Aapo, 2008. Modeling of surface UV radiation using satellite data. 109 p.

71. Leskinen, Ari, 2008. Experimental studies on aerosol physical properties and transformation in environmental chambers. 116 p.

72. Tarvainen, Virpi, 2008. Development of biogenetic VOC emission inventories for the boreal forest. 137 p.

73. Lohila, Annalea, 2008. Carbon dioxide exchange on cultivated and afforested boreal peatlands. 110 p.

74. Saarikoski, Sanna, 2008. Chemical mass closure and source-specific composition of atmospheric particles. 182 p.

75. Pirazzini, Roberta, 2008. Factors controlling the surface energy budget over snow and ice. 141 p.

76. Salonen, Kirsti, 2008. Towards the use of radar winds in numerical weather prediction. 87 p.

77. Luojus, Kari, 2009. Remote sensing of snow-cover for the boreal forest zone using microwave radar. 178 p.

78. Juusola, Liisa, 2009. Observations of the solar wind-magnetosphere-ionosphere coupling. 167 p.

79. Waldén, Jari, 2009. Meteorology of gaseous air pollutants. 177 p.

80. Mäkelä, Jakke, 2009. Electromagnetic signatures of lightning near the HF frequency band. 152 p.

81. Thum, Tea, 2009. Modelling boreal forest CO_2 exchange and seasonality. 140 p.

82. Lallo, Marko, 2010. Hydrogen soil deposition and atmospheric variations in the boreal zone. 91 p.

83.   Sandroos, Arto, 2010. Shock acceleration in the solar corona. 116 p.

84.   Lappalainen, Hanna, 2010. Role of temperature in the biological activity of a boreal forest. 107 p.

85.   Mielonen, Tero, 2010. Evaluation and application of passive and active optical remote sensing methods for the measurement of atmospheric aerosol properties. 125 p.